DOE/NASA CONTRACTOR REPORT

DOE/NASA CR-161539

SOLAR ENERGY SYSTEM PERFORMANCE EVALUATION - SEASONAL REPORT FOR COLT YOSEMITE, YOSEMITE NATIONAL PARK, CALIFORNIA

Prepared by

IBM Corporation
Federal Systems Division
150 Sparkman Drive
Huntsville, Alabama 35805

Under Contract NAS8-32036 with

National Aeronautics and Space Administration
George C. Marshall Space Flight Center, Alabama 35812

For the U. S. Department of Energy

U.S. Department of Energy

Solar Energy

TABLE OF CONTENTS

LIST OF FIGURES AND TABLES

1. FOREWORD

This Solar Energy System Performance Evaluation - Seasonal Report has been developed for the George C. Marshall Space Flight Center as a part of the Solar Heating and Cooling Development Program funded by the Department of Energy. The analysis contained in this document describes the technical performance of an Operational Test Site (OTS) functioning throughout a specified period of time which is typically one season. The objective of the analysis is to report the long term performance of the installed system and to make technical contributions to the definition of techniques and requirements for solar energy system design.

The contents of this document have been divided into the following topics of discussion:

- System Description
- Performance Assessment
- Operating Energy
- Energy Savings
- Maintenance
- Summary and Conclusions

Data used for the seasonal analyses of the Operational Test Site described in this document have been collected, processed and maintained under the OTS Development Program and have provided the major inputs used to perform the long term technical assessment.

The Seasonal Report document in conjunction with the Final Report for each Operational Test Site in the Development Program culminates the technical activities which began with the site selection and instrumentation system design in April 1976. The Final Report emphasizes the economic analysis of solar systems performance and features the payback performance based on life cycle costs for the same solar system in various geographic regions. Other documents specifically related to this system are References [1] through [5].*

*Numbers in brackets designate references found in Section 8.

2. SYSTEM DESCRIPTION

The Colt Yosemite Solar Energy System provides space heating for the visitors center at Yosemite National Park, California. The energy collection and storage subsystem consists of 980 square feet of liquid, flat plate collectors, a petroleum-based solar energy transport fluid, and a 2,500-gallon water filled storage tank. The collector array faces south at an angle of 50 degrees to the horizontal. A heat exchanger in the storage tank serves to transfer the collected solar energy to the water in the tank while isolating the transport fluid from the water in the tank. The collector fluid is designed to be stable under all temperature conditions. Solar heated water is pumped to a liquid-to-air heat exchanger within the space heating subsystem supply duct. If solar energy is not sufficient to meet the space heating demand, auxiliary hot water is provided from an oil-fired boiler to a second liquid-to-air heat exchanger within the space heating subsystem supply duct. The building's air circulation fan and motor-driven dampers distribute the energy to the building. The system, shown schematically in Figure 2-1, has four modes of operation. The sensor designations in Figure 2-1 are in accordance with NBSIR-76-1137 [6]. The measurement symbol prefixes: W, T, EP, I and F represent respectively: flow rate, temperature, electric power, insolation, and fossil fuel consumption. Figure 2-2 a pictorial of the Colt Yosemite Visitor's Center and Collector Array.

Mode 1 - Collector to Storage: This mode is initiated when the difference in temperature between the collector outlet and a temperature representative of the top of storage is 20°F or higher. The thermal transfer fluid is circulated through the collectors using circulating pump P1 to thermal storage and then recirculated to the collectors. Circulation continues in this mode until the difference between the collector outlet and top of storage is less than 3°F.

Mode 2 - Storage to Space Heating (Solar Only): This mode is initiated when there is a demand for space heating and the temperature in storage is greater than 105°F. Water from storage is circulated through a heat exchanger coil located in the heating supply duct using pump P2 and then returned to storage. The heating supply plenum fan transfers energy to the building. This mode continues until either thermal storage temperature drops below 105°F or the demand for space heating ceases.

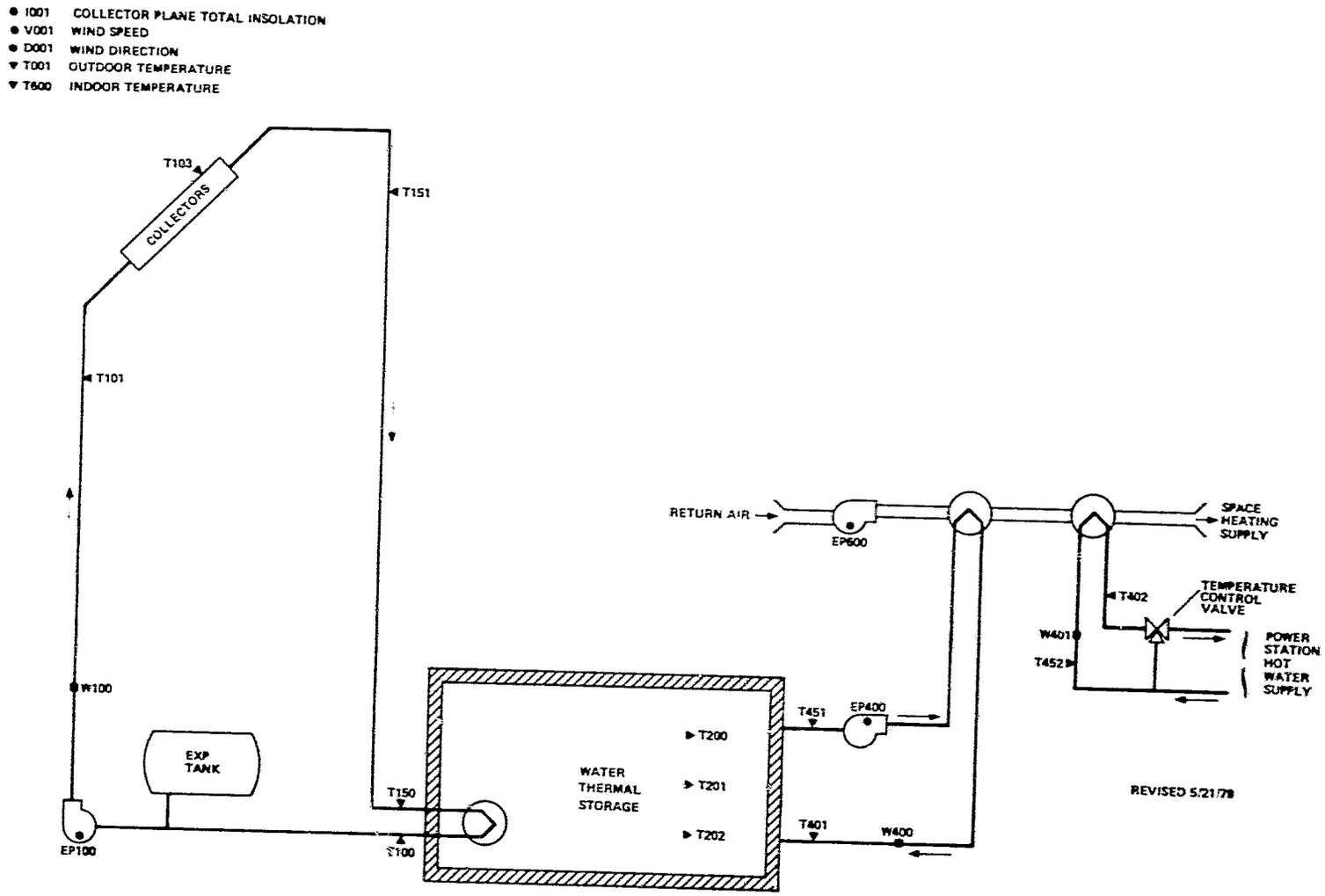

FIGURE 2-1 *COLT–YOSEMITE SOLAR ENERGY SYSTEM SCHEMATIC*

Mode 3 - Storage to Space Heating (Solar and Auxiliary): This mode is initiated when there is a demand for space heating, the temperature in storage is lower than 105°F, and the temperature delivered to the heat exchanger coil is greater than 90°F. Water from storage is circulated through the heat exchanger coil located in the heating supply duct using pump P2, and then returned to storage. The heating supply plenum fan transfers energy to the building. Stage two of the space heating thermostat activates the auxiliary furnace to supplement solar energy to satisfy the demand for heating. Circulation continues in this mode until thermal storage temperature drops below 90°F or the demand for space heating ceases.

Mode 4 - Conventional Heating: When solar energy for space heating is not available, (i.e., the storage temperature is less than 90°F), stage two of the space heating thermostat activates the auxiliary furnace to supply the required energy to satisfy the demand for heating. The heating supply plenum fan transfers energy to the building. Circulation continues in this mode until the demand for space heating ceases.

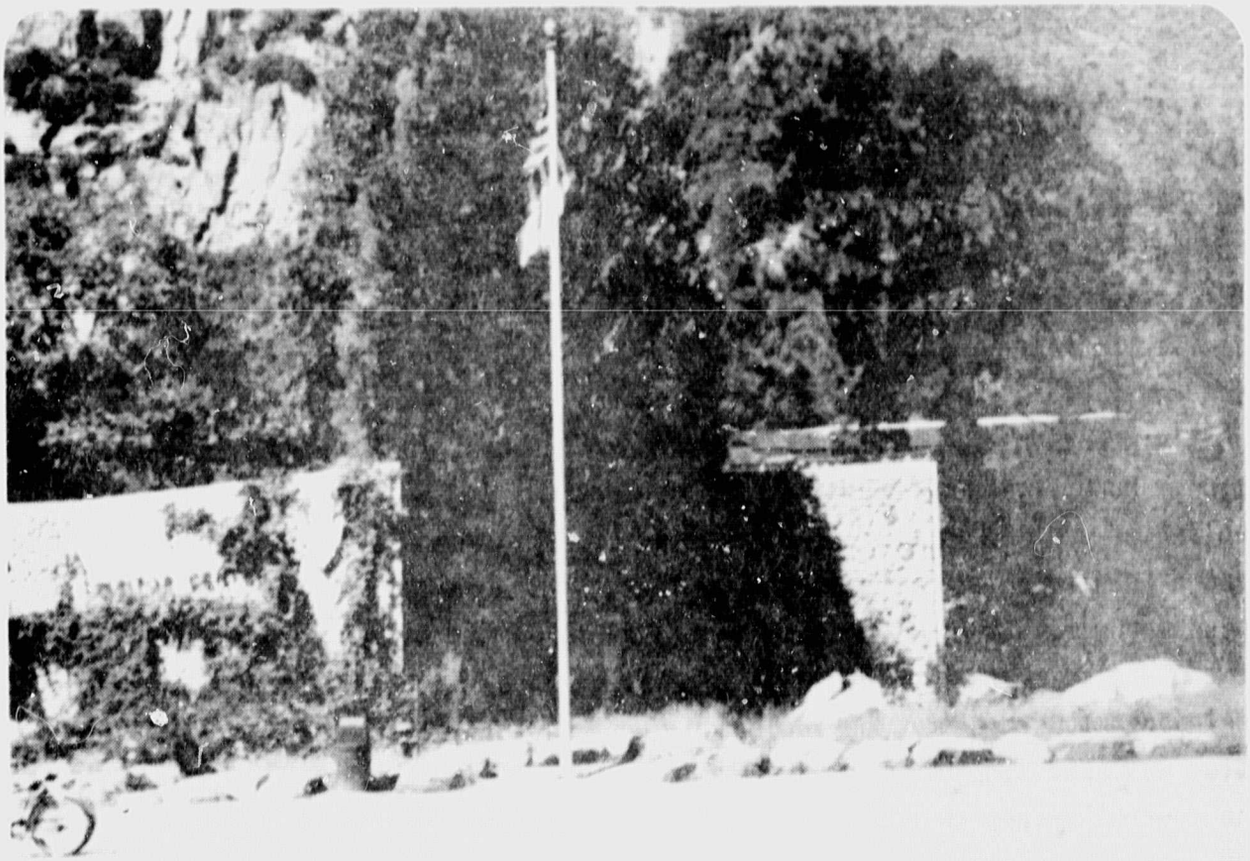

Figure 2-2 Colt-Yosemite Visitor's Center Pictorial

2.1 Typical System Operation

Curves depicting typical system operation on a cool bright day (November 19, 1979) are presented in Figures 2.1-1 (a) through 2.1-1 (e).

Figure 2.1-1 (a) shows the insolation on the collector array and the period when the array was operating (shaded area). On this particular day collector array initiation occurred at 0851 hours and operation continued until 1448 hours when it was shut down for the day. The insolation reached a peak value of 322 Btu/Hr-Ft^2 at 12:03 P.M.

Figure 2.1-1 (b), 2.1-1 (c), and 2.1-1 (d) show typical collector array temperatures during the day. During the early morning hours the collector array outlet temperature (T151), the collector array inlet temperature (T101) and the collector absorber plate temperature (T103) continued to decay from the temperatures achieved during the previous day's collection. As the sun started to rise at approximately 0747 hours T103 began to rise rapidly and reached 110°F before the system began normal operation at 0851 hours. It should be noted that T103 is not the control sensor that governs system operation. However, the absorber temperature (T103) is in close proximity to the collector control sensor and as such provides an accurate indication of collector plate temperatures in the vicinity of the control sensor. The actual system controls are set up such that a differential temperature of 20°F between the collector and storage is required before collected energy can be delivered to storage. The indicated differential temperature at array initiation was approximately 28.7°F which is greater than the expected value. However, no control system switching instabilities occurred.

During the operational period T103 generally tracked the insolation level except when the collector turn-on transient occurred. As would be expected absorber plate temperature reduced during the turn-on transient. The collector outlet temperature (T151) rose to a maximum value of 130°F at 1053 while the collector inlet temperature maximum was 115°F which occurred at the same time.

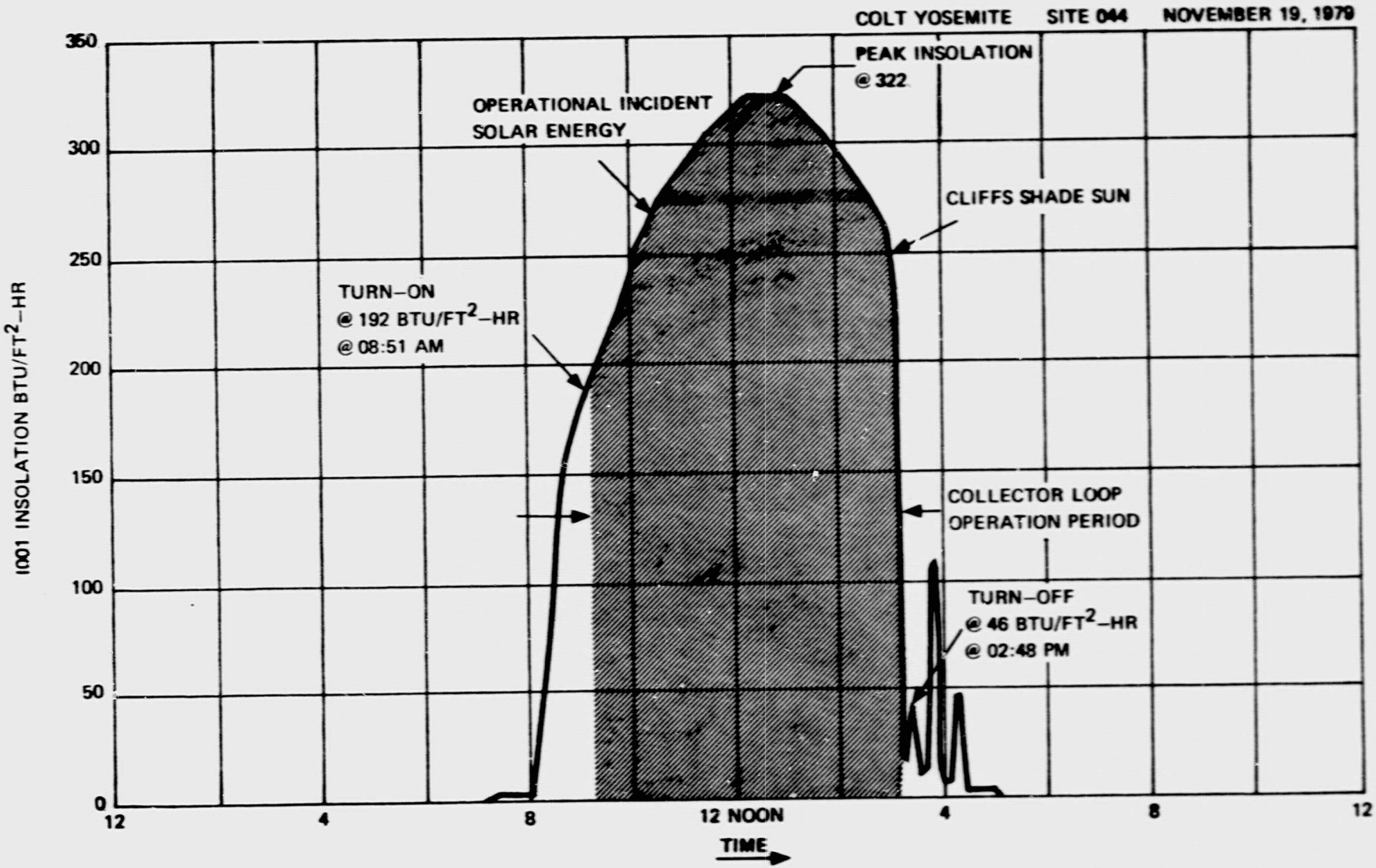

Figure 2.1-1(a) Solar Insolation Vs. Time of Day

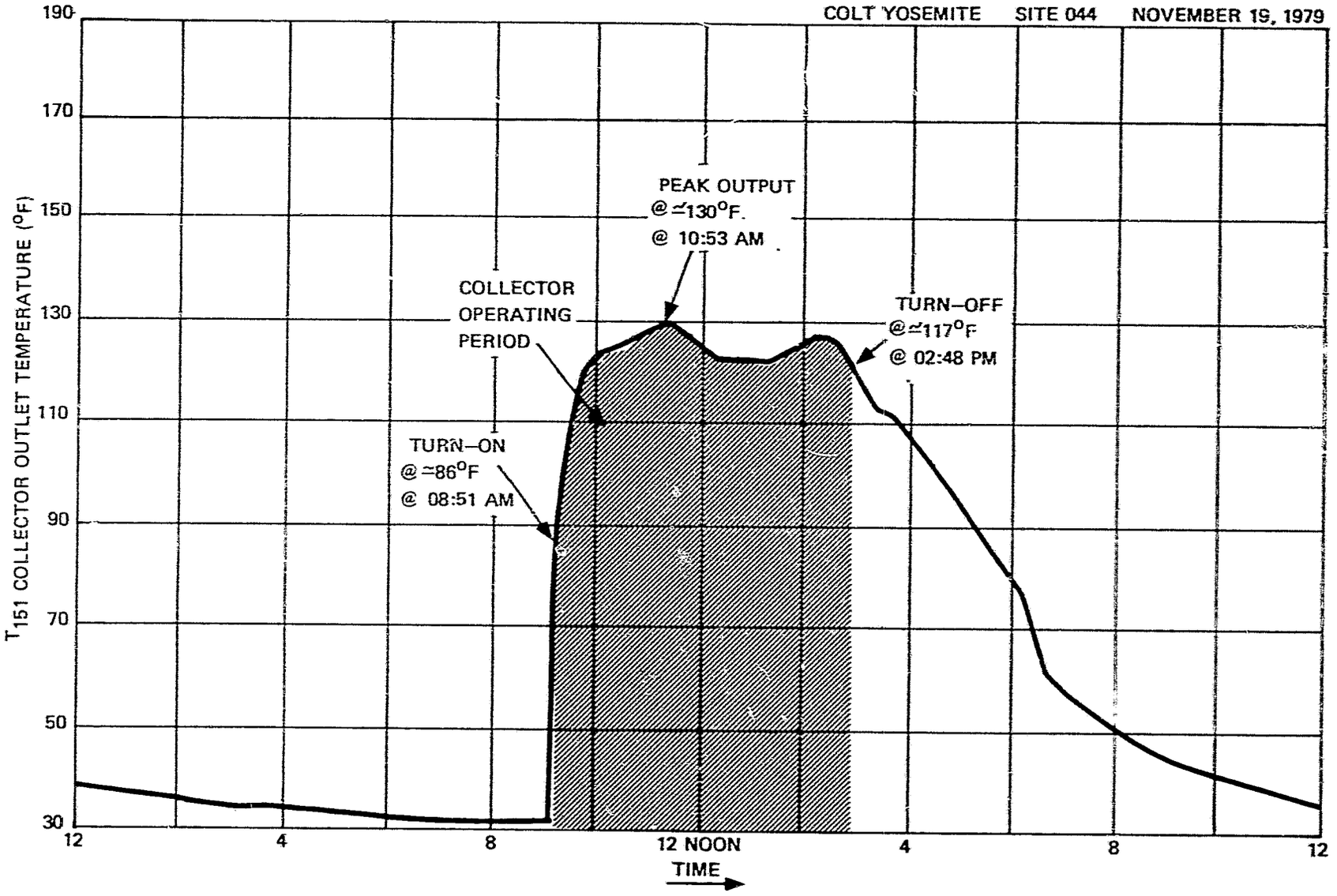

Figure 2.1-1(b) Collector Outlet Temperature Vs. Time of Day

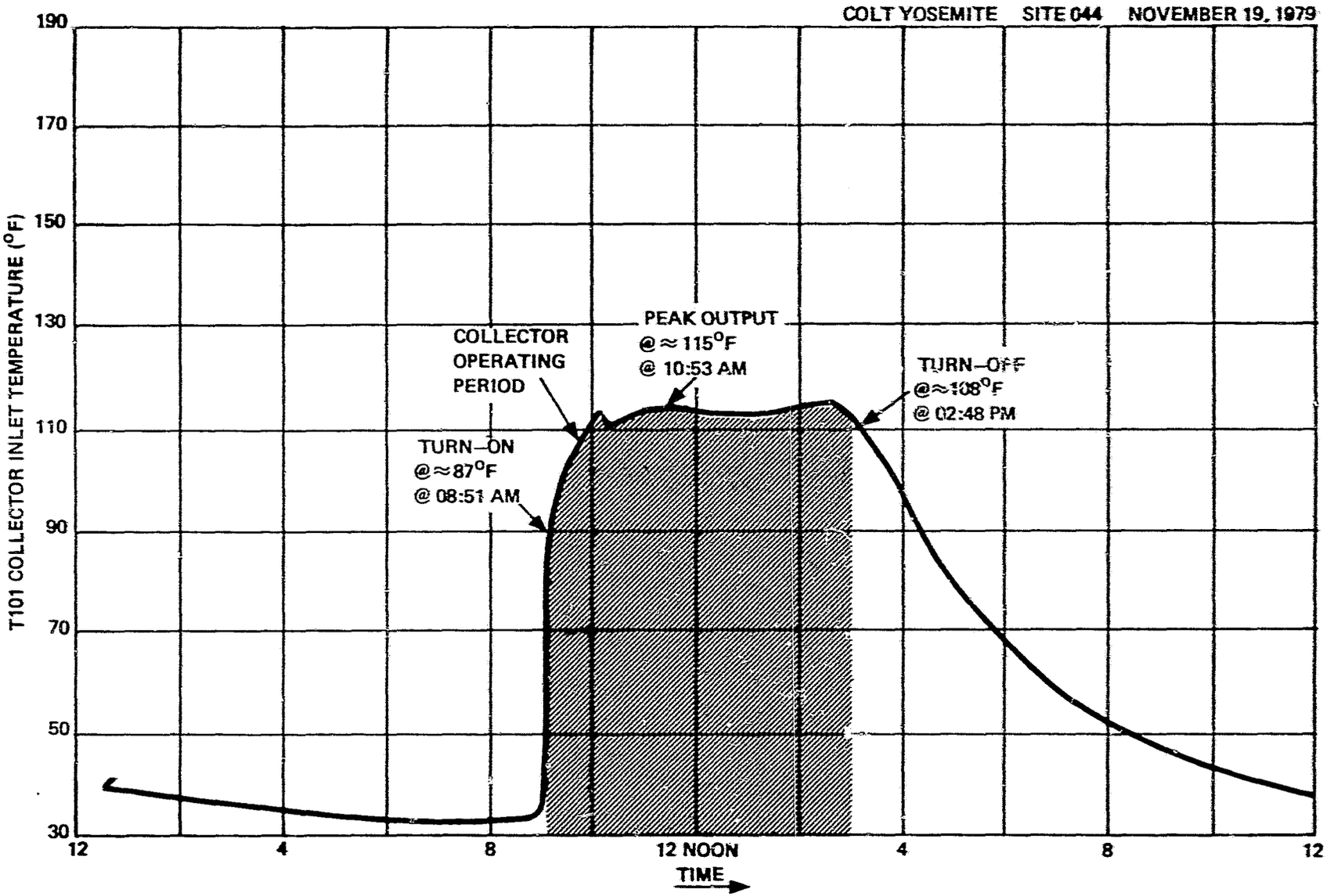

Figure 2.1-1(c) Collector Inlet Temperature Vs. Time of Day

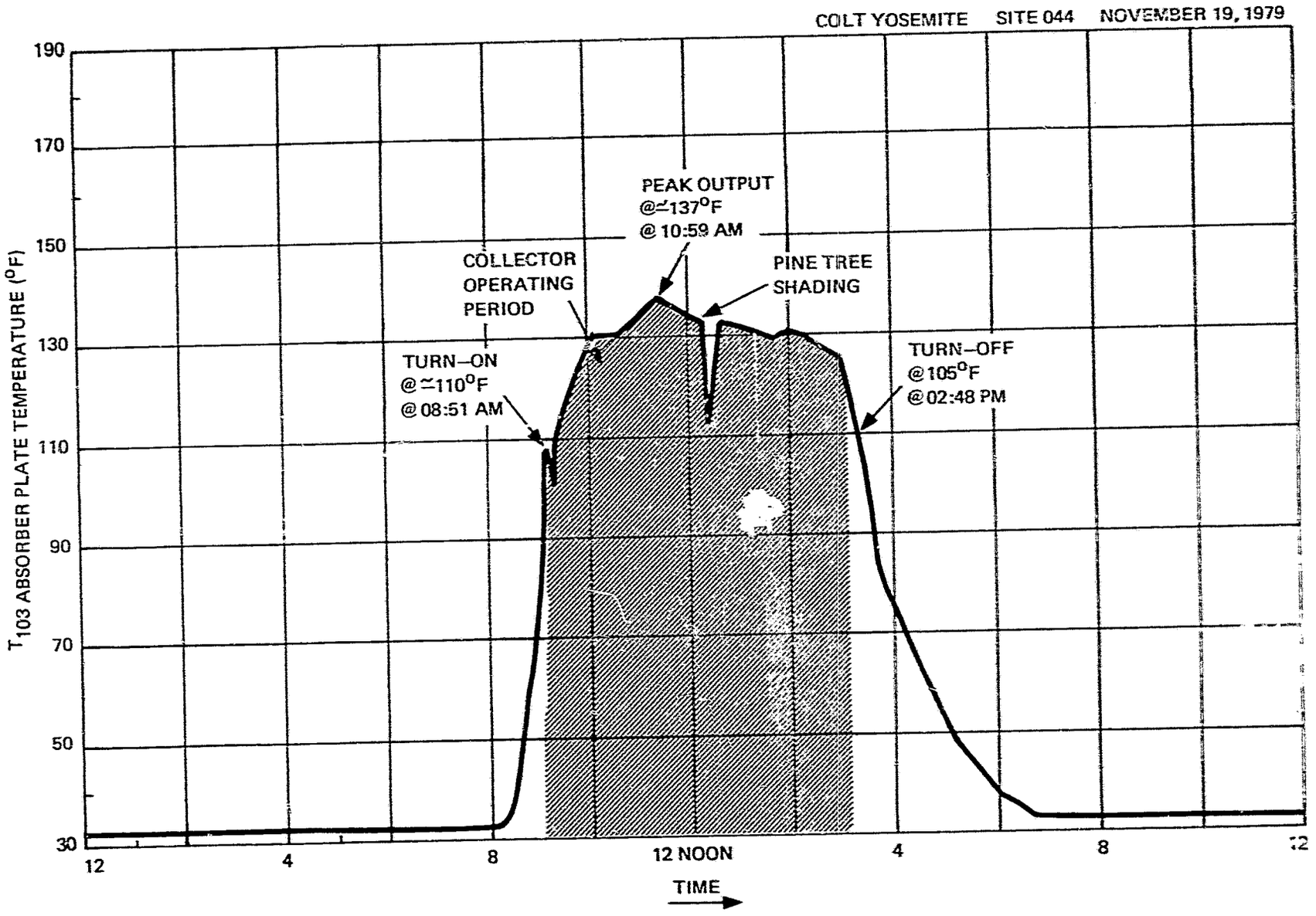

Figure 2.1-1( ) Absorber Temperature Vs. Time of Day

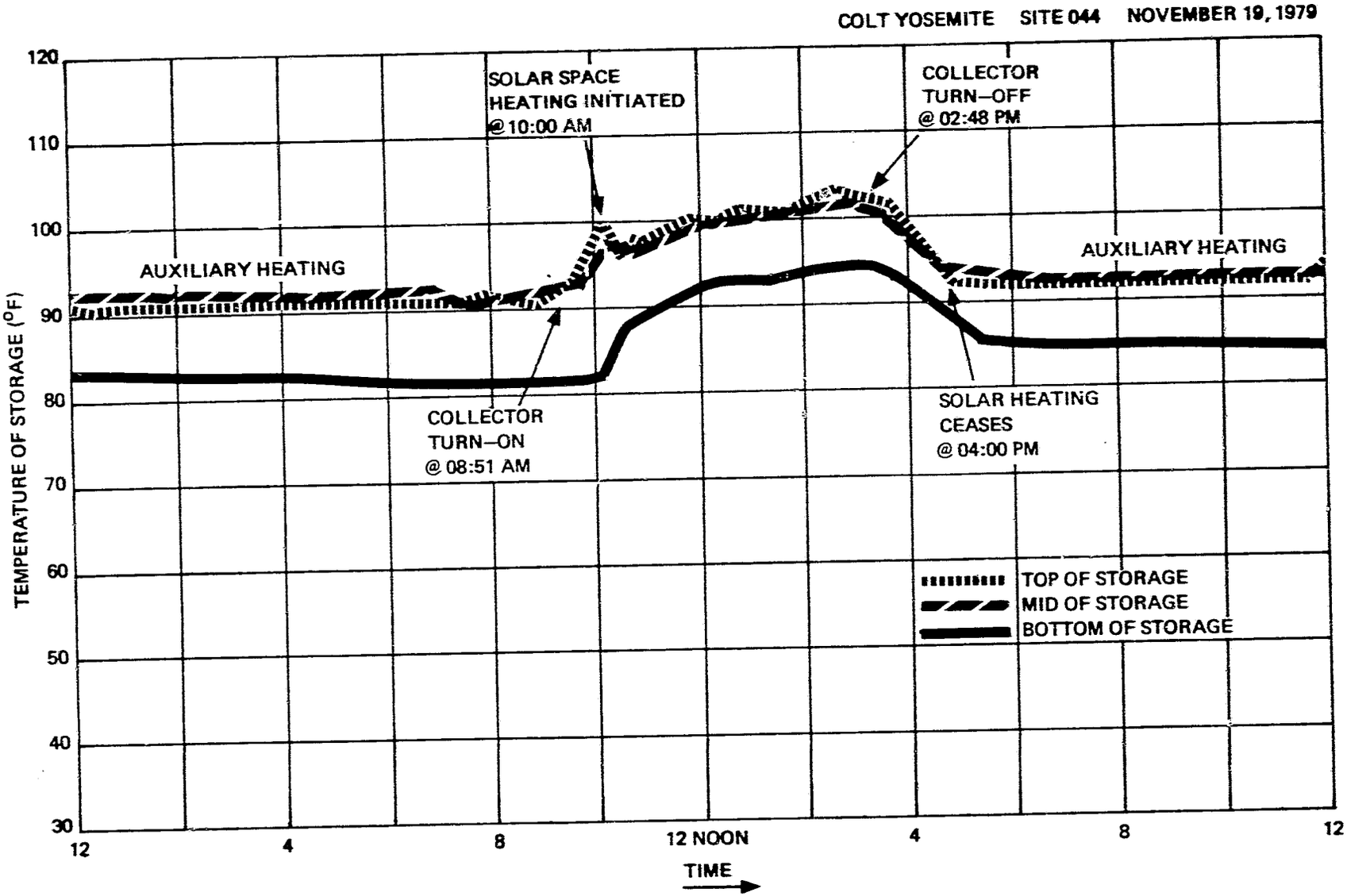

Figure 2.1-1(e) Storage Tank Temperature Profiles

The highest collector inlet and outlet differential temperature achieved was 14.2°F; and, correspondingly the highest collector outlet to storage temperature achieved was 32.1°F both of which occurred at 1053.

Collector array turn-off occurred at 1448 when the collector inlet to outlet temperature reduced below 7°F. The absorber to storage differential was 4°F. Again these temperature differentials are above the design temperature differential of 3°F; however, no control instabilities occurred. These operating temperature constraints are mentioned to make the reader aware that monitoring instrumentation and control sensors do not have direct correlation, but monitoring instrumentation can provide sufficient gross data to determine if each operational mode is functioning within a reasonable range of control temperature sensor limits.

Figure 2.1-1(e) shows the temperature profile of the 2,500-gallon liquid storage tank. During the early morning hours all space heating demands were satisfied with supplemental auxiliary energy. All available solar energy had been utilized to meet the space heating demand the previous day when storage temperatures dropped below 90°F. The solar storage subsystem is designed to supply all space heating energy requirements down to a storage temperature of 105°F and assist in meeting the demands down to a storage temperature of 90°F. Actually, solar supplied all of the demands down to a temperature of 93°F. The stability of the storage temperature subsequent to solar energy utilization is indicative of a very well insulated storage tank. After the collector array began operating at 0851, the storage tank began to warm up and continued to do so until 1000 when solar energy began meeting the space heating demand. Storage temperatures remained fairly stable because most of the energy was being utilized to meet the space heating demand. Later in the afternoon as ambient temperature rose, the storage tank temperature rose to a maximum of 102°F at collector array turn-off which occurred at 1448. After this time, solar satisfied most of the space demand until 1600 when storage temperatures dropped below 90°F. Auxiliary energy met the space heating demand the remainder of the day.

2.2 System Operating Sequence

Figure 2.2-1 presents bar charts showing typical system operating sequences for November 19, 1979. This data correlates with the curves presented in Figures 2.1-1 (a) through (e).

The most interesting observation that can be made from Figure 2.2-1 relates to the use of space heating auxiliary energy. The auxiliary subsystem was enabled the previous day when storage temperatures dropped below 105°F. At the time of solar collection initiation, storage tank temperatures were below the threshold temperature, 90°F, necessary for solar energy space heating utilization. Auxiliary energy met the load demands until 10:00. After this time, all demands were met by solar energy from the solar storage tank until 1600 when storage temperatures dropped below 90°F. This is typical of this solar energy system. The solar system is capable of meeting the space heating demand only a few hours after collector turn-off on good solar days during the winter months. In spring and fall months when the space heating demand is reduced, the solar energy system performs in a more normal fashion providing solar energy on demand throughout the evening and morning hours of the subsequent day.

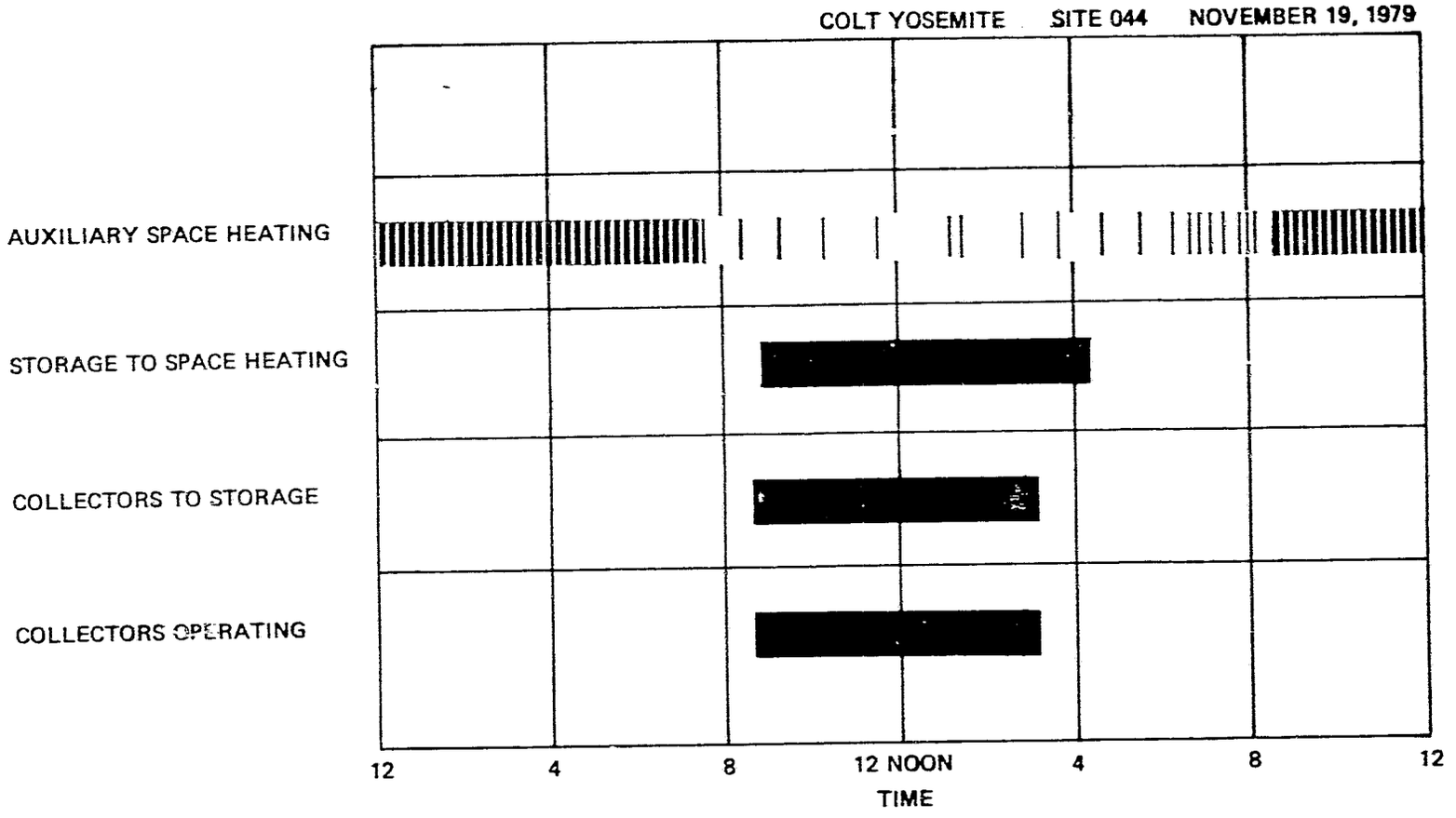

Figure 2.2-1 Typical System Operating Sequence

3. PERFORMANCE ASSESSMENT

The performance of the Colt Yosemite Solar Energy System has been evaluated for the May 1979 through April 1980 time period from two perspectives. The first was the overall system view in which the performance values of system solar fraction and net energy savings were evaluated against the prevailing and long term average climatic conditions and system loads. The second view presents a more in-depth look at the performance of the individual subsystems. Details relating to the performance of the system are presented first in Section 3.1 followed by the subsystem assessment in Section 3.2.

For the purposes of this solar energy system performance evaluation, monthly performance data were regenerated to reflect refinements and improvements in the system performance equations that were incorporated as the analysis period progressed. These modifications resulted in changes in the numerical values of some of the performance factors. However, the basic trends have not been affected.

Before beginning the discussion of actual solar energy system performance some highlights and pertinent information relating to site history are presented in the following paragraphs.

The Colt Yosemite Solar Energy System was initially brought on line in early September 1978. At that time all known system problems were addressed and corrected where possible. After the system was started up, a period of data monitoring was initiated to verify that the solar system and monitoring instrumentation were functioning properly.

During the monitoring period September 1978 until April 1980, several solar system operational deficiencies were present that affected overall solar system performance. Subsequent paragraphs will describe the operational difficulties and their effects on solar system performance.

The solar system is located in a valley of the Sierra Nevada mountains. The location is famous for its sheer walls and mountain peaks. In addition, large numbers of pine trees exist on the valley floor. These obstructions cause significant solar insolation shading to occur. The overall yearly reduction in insolation is approximately 18 percent. This situation will directly affect system performance and result in a 7 percent reduction in overall system performance (percentage reduction in insolation times collector operational efficiency).

The collector array was replaced twice during the monitoring period because of subsystem leakage. The original aluminum roll bond collectors were replaced in October 1978 with collectors of the same type. The collector array was again replaced with copper roll bond collectors beginning in September 1979 with completion occurring in early November 1979 when air was removed from the fluid transfer piping. The thermal transfer fluid was also changed to a less viscous fluid which permitted higher fluid flow. Also, several collector banks were turned off in December 1979 while the system was being repaired. Finally, three collectors were removed permanently in December 1979 and one in March 1980. These circumstances affect the amount of solar energy that could be collected during these months and hence the solar system performance. The overall reduction in solar system performance that can be expected because of these effects for the months October 1979 through April 1979 is approximately nineteen percent in October, five percent in December, three percent in January through March and 4 percent thereafter.

Heat transfer fluid flow through the auxiliary heat exchanger was found to be considerably below that expected. This necessitated changing the water flow meters twice to obtain sufficient accuracy. Even with the reduction in flow meter range, noise has a considerable effect on auxiliary consumption indications during periods when fluid flow is low. The low flow causes high differential temperatures to exist across the auxiliary heat exchanger. The combination of noise effects, low fluid flow and high differential temperatures

create some uncertainty as to how accurate auxiliary consumption measurement is being determined. No quantitative figure of performance degradation can be estimated for these effects.

The auxiliary water circulation pump failed in mid-January and was repaired in mid-February. During this period the auxiliary flow meter indication was incorrect and as such did not provide an accurate measurement of auxiliary consumption. This condition may have caused a considerable effect on solar system performance for that period and should be duly noted when considering the performance factor indications for January 1980 and February 1980.

Beginning in late December, the auxiliary flow indication began to become erratic. Prior to this time the auxiliary flow indication was in the order of 4 GPM and exhibited the expected half hour cycling characteristic of this subsystem when a substantial heating load exists. However, after December the auxiliary flow became more continuous at a lower level flow rate. The cause of this condition was later found to be the result of failure of the 3-way modulating valve (Figure 2-1) used to regulate flow to the auxiliary heat exchanger. This condition still exists. The reduced fluid flow has created a lower signal to noise ratio and as such has increased the uncertainty of the auxiliary flow measurement.

Because of the solar system deficiencies throughout the monitoring period September 1978 to April 1980, only the period May 1979 through April 1980 is considered representative of proper solar energy system performance. However, the performance degradations indicated in previous paragraphs must be considered when evaluating even this data. This seasonal report is based on solar system performance during this period.

3.1 System Performance

This Seasonal Report provides a system performance evaluation summary of the operation of the Colt-Yosemite Solar Energy System located in Yosemite National Park, California. This analysis was conducted by evaluation of measured system performance against the expected performance with long term average climatic conditions. The performance of the system is evaluated by calculating a set of primary performance factors which are based on those proposed in the intergovernmental agency report, "Thermal Data Requirements and Performance Evaluation Procedures for the National Solar Heating and Cooling Demonstration Program" [6]. The performance of the major subsystems is also evaluated in subsequent sections of this report.

The measurement data were collected for the period September 1978 through April 1980. However, the Seasonal Report is based on data collected between May 1979 and April 1980. This period represents the best indication of solar system performance. Before and after this evaluation period, the solar system was either inactive or not configured as designed. System performance data were provided through an IBM developed Central Data Processing System (CDPS) [7] consisting of a remote Site Data Acquisition (SDAS), telephone data transmission lines and couplers, an IBM System 7 computer for data management, and an IBM System 370/145 computer for data processing. The CDPS supports the collection and analysis of solar data acquired for instrumented systems located throughout the country. These data are processed daily and summarized into monthly performance formats which form a common basis for comparative system evaluation. These monthly summaries are the basis of the evaluation and data given in this report.

The solar energy system performance summarized in this section can be viewed as the dependent response of the system to certain primary inputs. This relationship is illustrated in Figure 3.1-1. The primary inputs are the incident solar energy, the outdoor ambient temperature and the system load. The dependent responses of the system are the system solar fraction and the total energy savings. Both the input and output definitions are as follows:

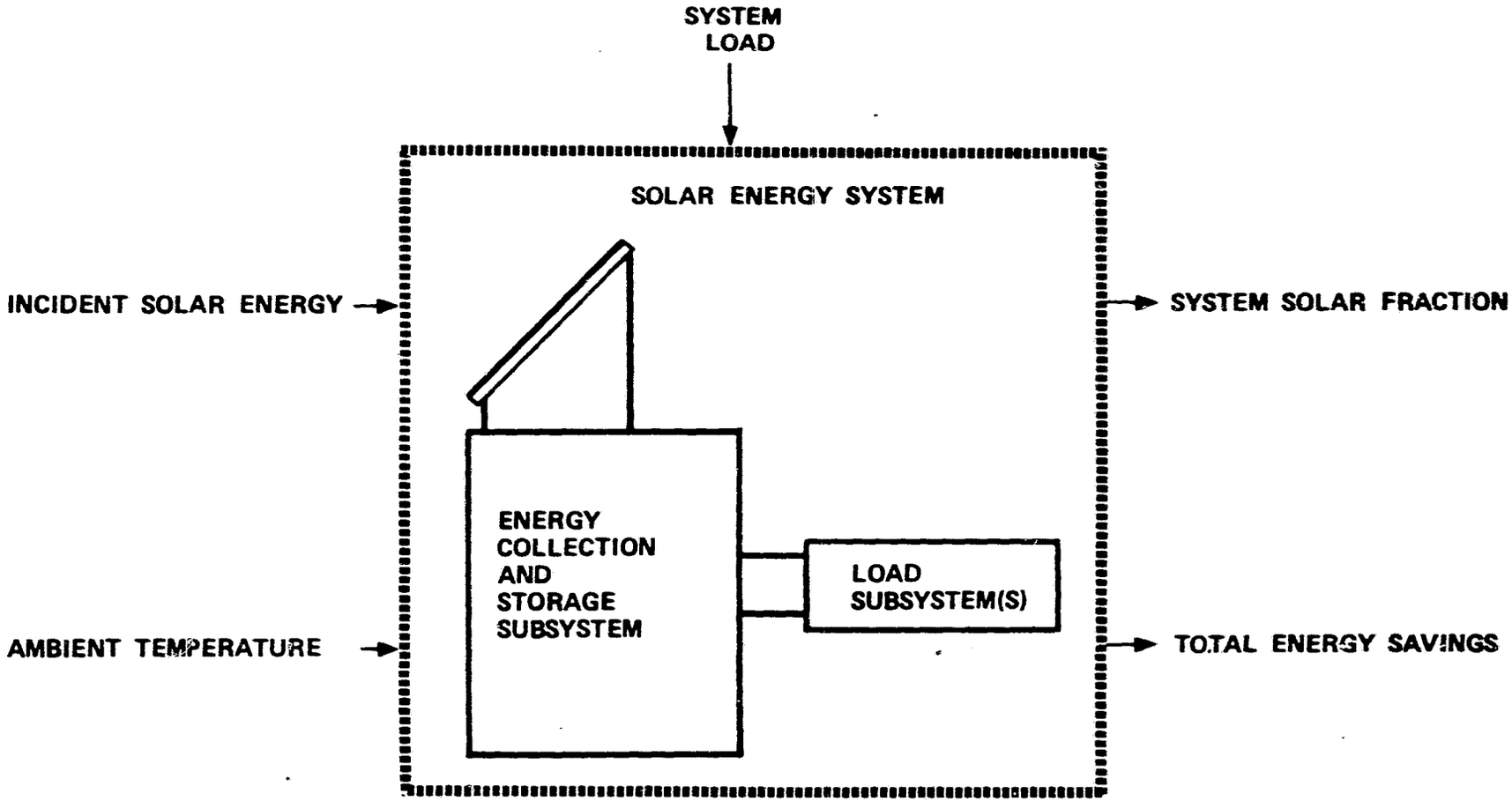

Figure 3.1-1 Solar Energy System Evaluation Block Diagram

Inputs

- Incident solar energy - The total solar energy incident on the collector array and available for collection.

- Ambient temperature - The temperature of the external environment which affects both the energy that can be collected and the energy demand.

- System load - The loads that the system is designed to meet, which are affected by the life style of the user (space heating/cooling, domestic hot water, etc., as applicable).

Outputs

- System solar fraction - The ratio of solar energy applied to the system loads to total energy (solar plus auxiliary energy) required by the loads.

- Total energy savings - The quantity of auxiliary energy (electrical or fossil) displaced by solar energy.

The monthly values of the inputs and outputs for the total operational period are shown in Table 3.1-1, the System Performance Summary. Comparative long-term average values of daily incident solar energy, and outdoor ambient temperature are given for reference purposes. The long-term data are taken from Reference 1 of Appendix C. Generally the solar energy system is designed to supply an amount of energy that results in a desired value of system solar fraction while operating under climatic conditions that are defined by the long-term average value of daily incident solar energy and outdoor ambient temperature. If the actual

TABLE 3.1-1

SYSTEM PERFORMANCE SUMMARY

COLT-YOSEMITE

Month	Daily Incident Solar Energy Per Unit Area (50° Tilt) (Btu/Ft^2-Day)			Ambient Temperature (°F)		System Load - Measured	Solar Fraction Percent		Total Energy Savings Fossil Equivalent at Source (Million Btu)
		Long-Term							
	Measured	No Shading	Shading	Measured	Long-Term Average	(Million Btu)	Measured	Expected	
May	1,746	2,061	1,699	59	58	9.44	85	72	12.10
Jun 79	1,705	2,051	1,696	66	64	3.52	100	97	4.13
Jul 79	1,596	2,048	1,778	72	68	0	0	0	0
Aug 79	1,601	2,194	1,987	70	67	0	0	0	0
Sep 79	1,837	2,301	2,076	70	64	1.66	100	54	2.92
Oct 79	1,781	2,090	1,890	56	56	15.60	41	68	8.23
Nov 79	1,261	1,857	1,517	44	47	49.03	19	15	11.73
Dec 79	1,104	1,535	1,079	41	40	39.87	20	15	9.92
Jan 80	919	1,541	1,108	41	39	36.38	19	12	8.92
Feb 80	1,054	1,792	1,231	44	43	33.47	21	16	9.36
Mar 80	1,529	2,087	1,672	44	46	47.77	11	11	3.83
Apr 80	1,541	2,129	1,733	51	52	40.49	18	24	9.75
Total	--	--		--	--	277.23	--	--	80.89
Average	1,473	1,974	1,622	55	54	23.10	23	22	6.74

climatic conditions are close to the long term average values, there is little adverse impact on the system's ability to meet design goals. This is an important factor in evaluating system performance and is the reason the long term average values are given. The data reported in the following paragraphs are taken from Table 3.1-1.

At the Colt-Yosemite site for the 12 month report period, the long-term average daily incident solar energy in the plane of the collector is estimated to be 1,622 Btu/Ft^2 when local shading is considered. The average daily measured value was 1,473 Btu/Ft^2 which is about nine percent below the long-term value. On a monthly basis, August of 1979 was the worst month with an average daily measured value of incident solar energy 19 percent below the long-term average daily value. May 1979 was the best month with an average daily measured value three percent above the long-term average daily value. On a long term basis it is obvious that the insolation is somewhat lower than normal but the good and bad months almost average out so that the long-term average performance should not be adversely influenced by small differences between measured and long-term average incident solar energy.

The outdoor ambient temperature influences the operation of the solar energy system in two important ways. First the operating point of the collectors and consequently the collector efficiency or energy gain is determined by the difference in the outdoor ambient temperature and the collector inlet temperature. This will be discussed in greater detail in Section 3.2.1. Secondly the load is influenced by the outdoor ambient temperature. The long-term average daily ambient temperature for the period from May 1979 through April 1980 was 54°F at the Colt-Yosemite site. This compares favorably with the measured value of 55°F. Thus, the actual heating load during the reporting period should be close to the long-term averages.

The system load has an important affect on the system solar fraction and the total energy savings. If the load is small and sufficient energy is available from the collectors, the system solar fraction can be expected to be large. However, the total energy savings will be less than under more nominal load conditions. This is illustrated by comparing the performance of the system during the spring and fall (May, June, September and October) and the winter (December, January, and February) months. The system solar fraction was higher than expected in the summer months and near that expected in the winter months.

Also presented in Table 3.1-1 are the measured and expected values of system solar fraction where system solar fraction is the ratio of solar energy applied to system loads to the total energy (solar plus auxiliary) applied to the loads. The expected values have been derived from a modified f-Chart analysis which uses measured weather and subsystem loads as inputs (f-Chart is the designation of a procedure that was developed by the Solar Energy Laboratory, University of Wisconsin, Madison, for modeling and designing solar energy systems [11]). The model used in the analysis is based on manufacturers' data and other known system parameters. The basis for the model is a set of empirical correlations developed for liquid and air solar energy systems that are presented in graphical and equation form and referred to as the f-Charts, where 'f' is a designator for the system solar fraction. The output of the f-Chart procedure is the expected system solar fraction. The measured value of system solar fraction was computed from measurements, obtained through the instrumentation system, of the energy transfers that took place within the solar energy system. These represent the actual performance of the system installed at the site.

The measured value of system solar fraction can generally be compared with the expected value so long as the assumptions which are implicit in the f-Chart procedure reasonably apply to the system being analyzed. As shown in Table 3.1-1, the measured system solar fraction of 23 percent was near the expected value of 22 percent generated by the modified f-Chart program. The overall performance estimate derived by the contractor [Colt, Inc.] predicted a solar fraction of 56 percent [1]. The building heat loss (3488 Btu/hr°F) expected for the visitor center combined with the maximum possible solar system performance cannot approach the contractors expected performance. However,

if the solar system had operated as designed with no performance degradations, the performance would have achieved a solar fraction near 28 percent. This performance would have been acceptable. Considering the substantial solar losses as contributing to the space heating demands, the solar system performance could be further enhanced to around 36 percent.

The total energy savings is the most important performance parameter for the solar energy system because the fundamental purpose of the system is to replace expensive conventional energy sources with less expensive solar energy. In practical consideration, the system must save enough energy to cover both the cost of its own operation and to repay the initial investment for the system. In terms of the technical analysis presented in this report the net total energy savings should be a significant positive figure. The total computed energy savings for the Colt-Yosemite solar energy system was 80.89 million Btu, or 578 gallons of fuel oil, which was a significant amount of energy. This is further illustrated by the 23 percent solar fraction of the measured heating demands achieved by the system. However, this savings is based only on measured inputs of solar energy to the load subsystems. At the Colt-Yosemite site there were a significant amount of uncontrolled (and hence unmeasured) inputs of solar energy into the building. These uncontrolled inputs of solar energy came primarily from transport losses and tended to reduce the overall heating load, which in turn tended to increase real savings. This situation is addressed in more detail in the appropriate sections that follow.

3.2 Subsystem Performance

The Colt-Yosemite Solar Energy Installation may be divided into three subsystems:

1. Collector array
2. Storage
3. Space heating

Each subsystem has been evaluated by the techniques defined in Section 3 and is numerically analyzed each month for the monthly performance assessment. This section presents the results of integrating the monthly data available on the three subsystems for the period May 1979 through April 1980.

3.2.1 Collector Array Subsystem

Two different types of collectors were utilized in the Colt-Yosemite Solar Energy System. The first Colt-Yosemite collector array consisted of forty-two Colt A-151 series flat-plate liquid collectors all connected in parallel. These collectors were aluminum roll bond type with a single glazing and a selective absorber plate coating which also incorporates a "waffle" flow path design. The viscosity of the petroleum-based thermal energy transport fluid (Shell 33) and variable collector inlet temperatures resulted in a total collector array flow which varied from 13 GPM in winter to 38 GPM in summer. The first collector array was in place between September 1978 and June 1979.

The second collector array also consists of forty-two Colt A-151 series flat-plate collectors all connected in parallel. However, these collectors are copper roll bond type with a black paint absorber plate coating which also incorporates an integral tube flow path design. The viscosity of the petroleum-based thermal energy transport fluid (DIALA-AX oil) and variable collector inlet temperatures result in a total collector array flow which varies from 46 GPM in winter to 50 GPM in spring and fall months.

The collector array arrangement for both types is shown pictorially in Figure 3.2.1-1 (a). Details of the collector array liquid flow paths are shown in Figure 3.2.1-1 (b). The collector subsystem analysis and data are given in the following paragraphs.

Collector array performance is described by the collector array efficiency. This is the ratio of collected solar energy to incident solar energy, a value always less than unity because of collector losses. The incident solar energy may be viewed from two perspectives. The first assumes that all available solar energy incident on the collectors must be used in determining collector array efficiency. The efficiency is then expressed by the equation:

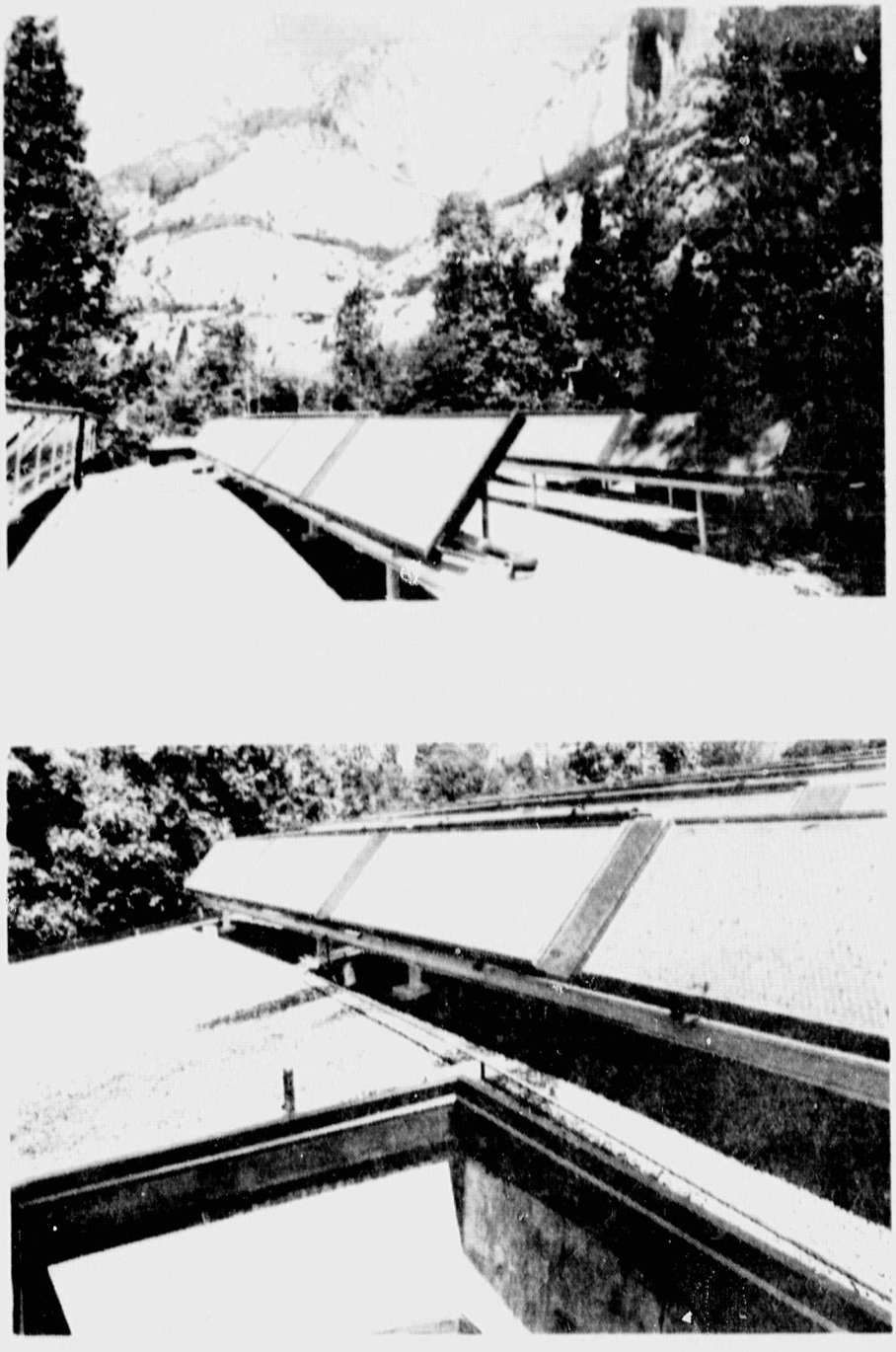

Figure 3.2.1-1(a) Collector Arrangement

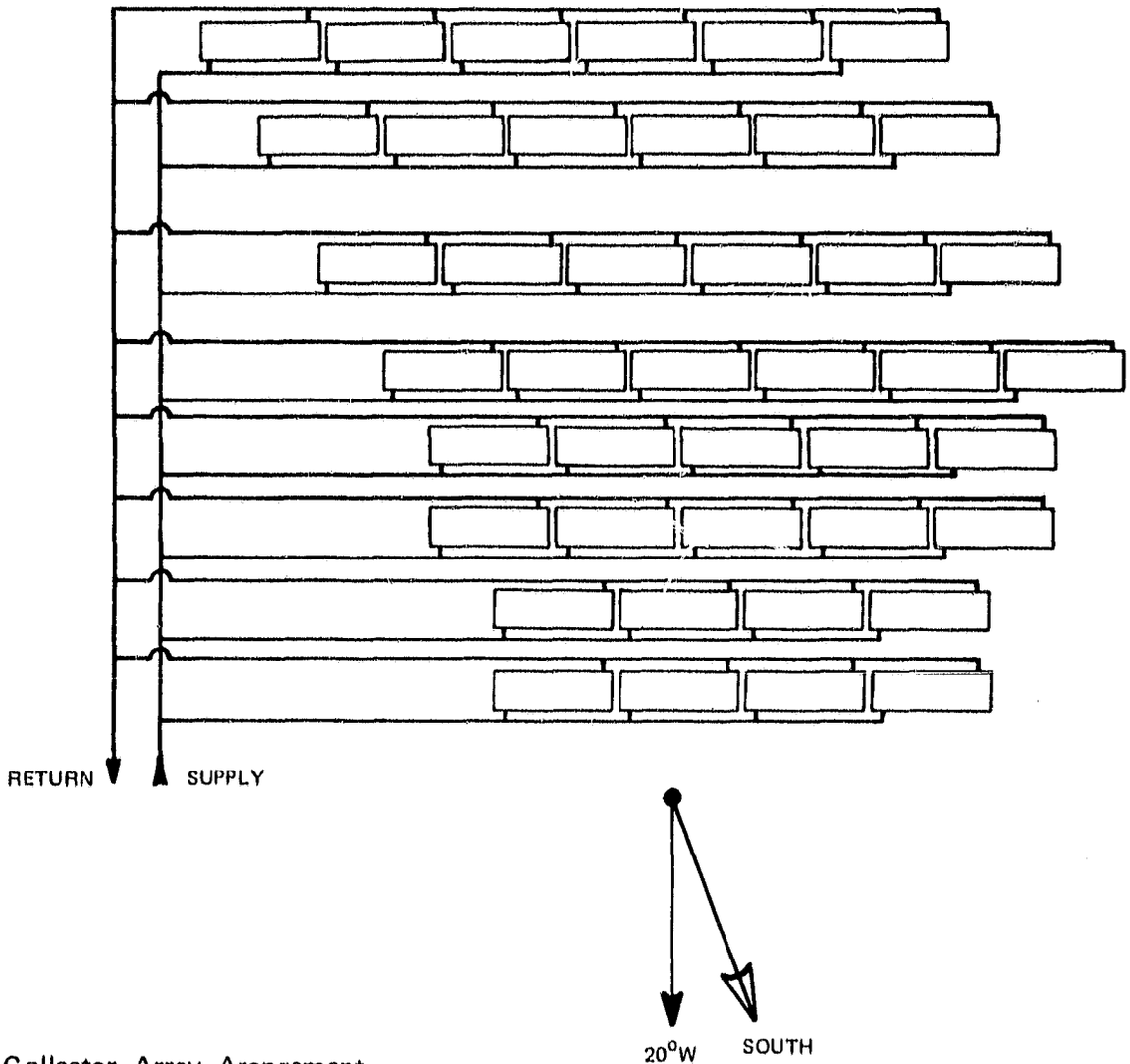

Collector Array Arangement

COLLECTOR ARRAY		SITE LOCATION	
TILT	– 50°	LATITUDE	– 36.77N
AZIMUTH	– 20°West of South	LONGITUDE	– 119.72W

Figure 3.2.1-1(b) Collector Details

$$\eta_c = Q_s/Q_i \quad (1)$$

where η_c = Collector array efficiency

Q_s = Collected solar energy

Q_i = Incident solar energy

The efficiency determined in this manner includes the operation of the control system. For example, solar energy can be available at the collector, but the collector absorber plate temperature may be below the minimum control temperature set point for collector loop operation, thus the energy is not collected. The monthly efficiency by this method is listed in the column entitled "Collector Array Efficiency" in Table 3.2.1-1.

The second viewpoint assumes that only the solar energy incident on the collector when the collector loop is operational be used in determining the collector array efficiency. The value of the operational incident solar energy used is multiplied by the ration of the gross collector area to the gross collector array area to compensate for the difference between the two areas caused by installation spacing. The efficiency is then expressed by the equation:

$$\eta_{co} = Q_s/(Q_{oi} \times A_p/A_a) \quad (2)$$

where η_{co} = Operational collector array efficiency

Q_s = Collected solar energy

Q_{oi} = Operational incident solar energy

A_p = Gross collector area (the product of the number of collectors and the envelope area of one collector)

A_a = Gross collector array area (total area including all mounting and connecting hardware and spacing of units)

The monthly efficiency computed by this method is listed in the column entitled "Operational Collector Array Efficiency" in Table 3.2.1-1.

In the ASHRAE Standard 93-77 [8] a collector efficiency is defined in the same terminology as the operational collector array efficiency. However, the ASHRAE efficiency is determined from instantaneous evaluation under tightly controlled, steady state test conditions, while the operational collector array efficiency is determined from actual dynamic conditions of daily solar energy system operation in the field.

The ASHRAE Standard 93-77 definitions and methods often are adopted by collector manufacturers and independent testing laboratories in evaluating collectors. The collector evaluation performed for this report using the field data indicates that there was a significant difference between the laboratory single panel collector data and the collector data determined from long-term field measurements. This may or may not always be the case, and there are two primary reasons for differences when they exist:

- Test conditions are not the same as conditions in the field, nor do they represent the wide dynamic range of field operation (i.e., inlet and outlet temperature, flow rates and flow distribution of the heat transfer fluid, insolation levels, aspect angle, wind conditions, etc.).

- Collector tests are not generally conducted with units that have undergone the effects of aging (i.e. changes in the characteristics of the glazing

TABLE 3.2.1-1

COLLECTOR ARRAY PERFORMANCE

Month	Incident Solar Energy (Million Btu)	Collected Soler Energy (Million Btu)	Collector Array Efficiency	Operational Incident Energy (Million Btu)	Operational Collector Array Efficiency
May 79	53.04	11.91	0.23	39.45	0.30
Jun 79	50.14	4.91	0.10	18.60	0.26
Jul 79	48.47	0	0	0	0
Aug 79	48.64	0	0	0	0
Sep 79	54.02	3.68	0.07	10.58	0.35
Oct 79	53.34	7.48	0.14	23.52	0.32
Nov 79	37.06	13.07	0.35	32.99	0.40
Dec 79	33.06	11.04	0.33	29.63	0.37
Jan 80	25.93	9.33	0.36	21.05	0.44
Feb 80	27.81	9.85	0.35	22.68	0.43
Mar 80	42.25	13.38	0.33	33.38	0.40
Apr 80	41.01	9.43	0.23	25.12	0.38
Total	514.77	94.08	--	257.00	--
Average	42.90	7.84	0.23*	21.42	0.37

*Computed using collector operational months.

material, collection of dust, soot, pollen or other foreign material on the glazing, deterioration of the absorber plate surface treatment, etc.)

Consequently field data collected over an extended period will generally provide an improved source of collector performance characteristics for use in long-term system performance definition.

The long-term data base for Colt-Yosemite includes the months from September 1978 through April 1980. Although the solar energy system was in operation for most of the period, the solar system operated as designed only between February 1979 and April 1980. Data system problems and a change of collectors prevent analyzing collector performance over an entire heating season. Thus, the intervals between February 1979 and May 1979 and February 1980 and May 1980 were chosen as the collector evaluation periods. All collector operating conditions were stable during these periods and no data problems existed.

The operational collector array efficiency data given in Table 3.2.1-1 are monthly averages based on instantaneous efficiency computations over the seasonal report performance period using all available data. For detailed collector analysis it was desirable to use a limited subset of the available data that characterized collector operation under "steady state" conditions. This subset was defined by applying the following restrictions:

(1) The measurement period was restricted to collector operation when the sun angle was within 30 degrees of the collector normal.

(2) Only measurements associated with positive energy gain from the collectors were used, i.e., outlet temperatures must have exceeded inlet temperatures.

(3) The sets of measured parameters were restricted to those where the rate of change of all parameters of interest during two regular data system intervals* was limited to a maximum of 5 percent.

Instantaneous efficiencies (n_j) computed from the "steady state" operation measurements of incident solar energy and collected solar energy by Equation (2)** were correlated with an operating point determined by the equation:

$$x_j = \frac{T_i - T_a}{I} \qquad (3)$$

where x_j = Collector operating point at the j^{th} instant

T_i = Collector inlet temperature

T_a = Outdoor ambient temperature

I = Rate of incident solar radiation

The data points (n_j, x_j) were then plotted on a graph of efficiency versus operating point and a first order curve described by the slope-intercept formula was fitted to the data through linear regression techniques. The form of this fitted efficiency curve is:

*The data system interval was 5-1/3 minutes in duration. Values of all measured parameters were continuously sampled at this rate throughout the performance period.

**The ratio A_p/A_a is assumed to be unity for this analysis.

$$\eta_j = b - mx_j \qquad (4)$$

where η_j = Collector efficiency corresponding to the j^{th} instant

b = Intercept on the efficiency axis

$(-)m$ = Slope

x_j = Collector operating point at j^{th} instant

The relationship between the empirically determined efficiency curve and the analytically developed curve will be established in subsequent paragraphs.

The analytically developed collector efficiency curve is based on the Hottell-Whillier-Bliss equation

$$\eta = F_R(\tau\alpha) - F_R U_L \left(\frac{T_i - T_a}{I} \right) \qquad (5)$$

where η = Collector efficiency

F_R = Collector heat removal factor

τ = Transmissivity of collector glazing

α = Absorptance of collector plate

U_L = Overall collector energy loss coefficient

T_i = Collector inlet fluid temperature

T_a = Outdoor ambient temperature

I = Rate of incident solar radiation

The correspondence between equations (4) and (5) can be readily seen. Therefore by determining the slope-intercept efficiency equation from measurement data, the collector performance parameters corresponding to the laboratory single panel data can be derived according to the following set of relationships:

$$b = F_R(\tau\alpha)$$
$$\text{and} \qquad (6)$$
$$m = F_R U_L$$

where the terms are as previously defined

The discussion of the collector array efficiency curves in subsequent paragraphs is based upon the relationships expressed in Equation (6). However, the single panel curve is not representative of the collector array performance expected of this system. The collector/storage loop contains a heat exchanger in the storage tank. The heat exchanger modifies the collector performance [4, 5]. A heat exchanger modifier (penalty factor) F_R'/F_R (fraction of $F_R U_L$) was determined by MSFC from laboratory test results and/or from contractor information. F_R'/F_R is a function of the heat exchanger effectiveness, collector/storage loop capacitance rates and collector array area. Proper sizing of these parameters should result in a F_R'/F_R value greater than 0.90, or a maximum 10 percent energy penalty over the no heat exchanger systems. The F_R'/F_R penalty factor for Colt Yosemite was determined to be 0.874. The $F_R(\tau\alpha)$ and $F_R U_L$ terms are modified appropriately to account for this circumstance.

In deriving the collector array efficiency curves by the linear regression technique, measurement data over the entire performance period yields higher confidence in the results than similar analysis over shorter periods. Over the longer periods the collector array is forced to operate over a wider dynamic range. This eliminates the tendency shown by some types of solar energy systems* to cluster efficiency values over a narrow range of

* Single tank hot water systems show a marked tendency toward clustering because the collector inlet temperature remains relatively constant and the range of values of ambient temperature and incident solar energy during collector operation are also relatively restricted on a short-term basis.

operating points. The clustering effect tends to make the linear regression technique approach constructing a line through a single data point. The use of data from the entire performance period results in a collector array efficiency curve that is more accurate in long-term solar system performance prediction. The long-term curve for the aluminum collectors, the curve derived from the laboratory single panel data, and the modified laboratory panel curve are shown in Figure 3.2.1-2 (ε). The long-term first order curve shown in Figure 3.2.1-2 (a) has a slightly greater negative slope than the curve derived from single panel laboratory test data. This is attributable to higher losses resulting from array effects. The laboratory predicted instantaneous efficiency is not in close agreement with the curve derived from actual field operation. This indicates that the laboratory derived curve might not be useful for design purposes in an array configuration of this type. However, the modified laboratory performance curve, which accounts for the heat exchanger in the collector loop, is in good agreement with the actual measured performance of the collector array. Therefore, the modified collector performance curve would be useful for design purposes when a heat exchanger is employed.

For information purposes the data associated with Figure 3.2.1-2 (a) is as follows:

Single panel laboratory data

$F_R(\tau\alpha) = 0.757$ $\qquad$ $F_RU_L = -1.177$

Modified performance estimate

$F_R(\tau\alpha) = 0.662$ $\qquad$ $F_RU_L = -1.029$

Long-term field data

$F_R(\tau\alpha) = 0.720$ $\qquad$ $F_RU_L = -1.224$

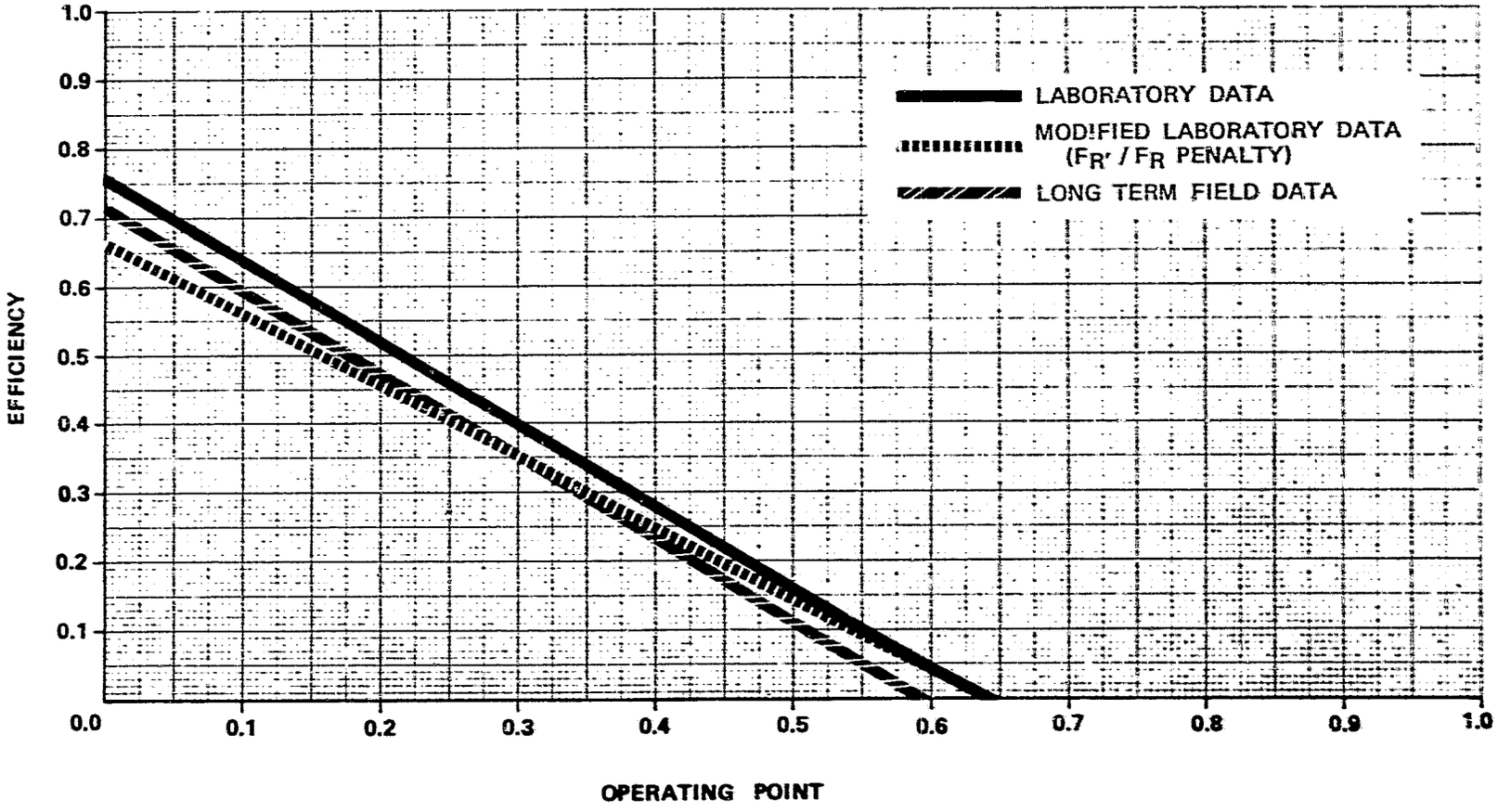

Figure 3.2.1-2(a) Colt Yosemite Collector Efficiency Curve-Aluminum Absorber

The long-term curve for the copper collectors, the curve derived from the laboratory single panel data, and the modified laboratory single panel curve are shown in Figure 3.2.1-2 (b). Again, the laboratory predicted instantaneous efficiency is not in close agreement with the curve derived from actual field operation. As can be seen, the instantaneous performance of both collector types are similar with the overall performance of the copper collector array being slightly superior to the aluminum collector array.

For informational purposes the data associated with figure 3.2.1-2 (b) is as follows:

Single Panel Laboratory Data:

$F_R(\tau\alpha) = 0.765$ $\qquad$ $F_RU_L = -1.269$

Modified Performance Estimate

$F_R(\tau\alpha) = 0.662$ $\qquad$ $F_RU_L = 1.109$

Long Term Field Data

$F_R(\tau\alpha) = 0.782$ $\qquad$ $F_RU_L = 1.412$

Table 3.2.1-2 presents data comparing the monthly measured values of solar energy collected with the predicted performance determined from the long-term regression curve and the laboratory single panel efficiency curve for both the aluminum and copper collector arrays. The predictions were derived by the following procedure:

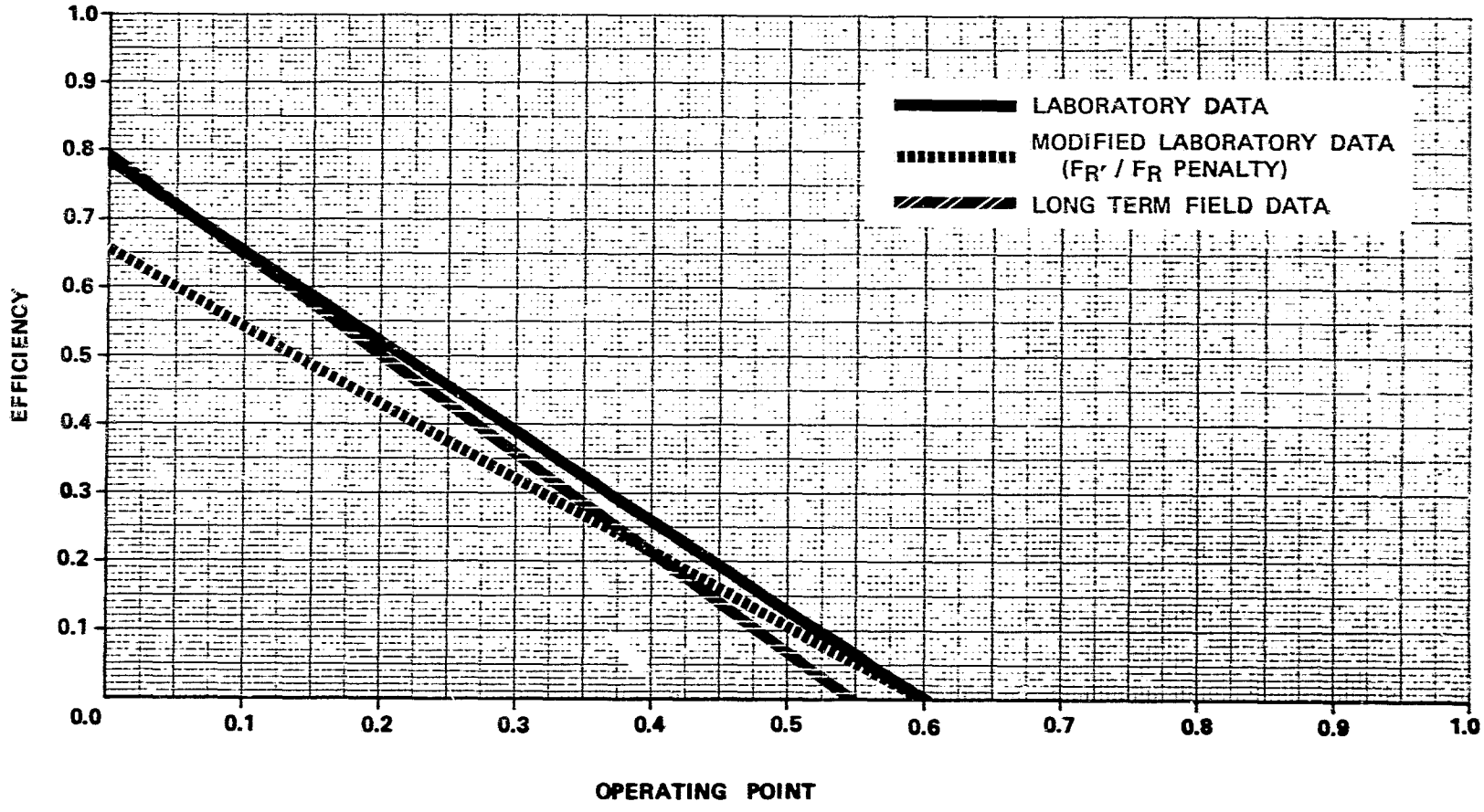

Figure 3.2.1-2(b) Colt Yosemite Collector Efficiency Curve-Copper Absorber

1. The instantaneous operating points were computed using Equation (3).

2. The instantaneous efficiency was computed using Equation (4) with the operating point computed in Step 1 above for:

   a. The long-term linear regression curve for collector array efficiency

   b. The laboratory single panel collector efficiency curve

3. The efficiencies computed in Steps 2a and 2b above were multiplied by the measured solar energy available when the collectors were operational to give two predicted values of solar energy collected.

The error data in Table 3.2.1-2 were computed from the differences between the measured and predicted values of solar energy collected according to the equation:

$$\text{Error} = (A-P)/P \qquad (7)$$

where A = Measured solar energy collected
P = Predicted solar energy collected

The computed error is then an indication of how well the particular prediction curve fitted the reality of dynamic operating conditions in the field.

TABLE 3.2.1-2

ENERGY GAIN COMPARISON

(ANNUAL)

SITE: COLT YOSEMITE YOSEMITE NATIONAL PARK, CALIFORNIA

Month	Collected Solar Energy (Million Btu)	Error	
		Field Derived Long-Term	Laboratory Single Panel
Feb 79	6.74	-0.128	-0.139
Mar 79	13.88	0.012	-0.036
Apr 79	17.54	0.011	-0.005
May 79	11.50	-0.151	-0.173
Average	12.39	-0.045	-0.070
Feb 80	9.32	-0.047	-0.115
Mar 80	13.04	0.001	-0.063
Apr 80	8.98	0.015	-0.059
May 80	4.69	0.027	-0.021
Average	9.00	-0.005	-0.070

The values of "Collected Solar Energy" given in Table 3.2.1-2 are not necessarily identical with the values of "Collected Solar Energy" given in Table 3.2.1-1. Any variations are due to the differences in data processing between the software programs used to generate the monthly performance assessment data and the component level collector analysis program. These data are shown in Table 3.2.1-2 only because they form the references from which the error data given in the table are computed.

The data from Table 3.2.1-2 illustrates that for the Colt-Yosemite site the average error computed from the difference between the measured solar energy collected and the predicted solar energy collected based on the field derived long-term collector array efficiency curve was -0.5 (4.5 percent for the aluminum collector array) percent for the copper collector array. For the curve derived from the laboratory single panel data, the error was -7 percent for both collector array types. Thus the long-term collector array efficiency curves give better results than the laboratory single panel curves. The long-term collector array efficiency curves are in closer agreement with the modified laboratory curves.

A histogram of collector array operating points illustrates the distribution of instantaneous values as determined by Equation (3) for the entire month. The histogram was constructed by computing the instantaneous operating point value from site instrumentation measurements at the regular data system intervals throughout the month, and counting the number of values within contiguous intervals of width 0.01 from zero to unity. The operating point histogram shows the dynamic range of collector operation during the month from which the midpoint can be ascertained. The average collector array efficiency for the month can then be derived by projecting the midpoint value to the appropriate efficiency curve and reading the corresponding value of efficiency.

Another characteristic of the operating point histogram is the shifting of the distribution along the operating point axis. This can be explained in terms of the characteristics of the system and the climatic factors of the site, i.e., incident solar energy and ambient temperature. Figure 3.2.1-3 shows two histograms that illustrate a typical winter month (March) and a typical summer month (June) operation of the aluminum collector array. The approximate average operating point for March is at 0.27 and for June at 0.47. This movement of the operating point is typical of the system. However, the operating point during winter months is essentially the same as the March operating point.

Also shown in Figure 3.2.1-3 on the March operating point histogram is the monthly collector array efficiency of 0.40 for March (Table 3.2.1-1) and the March field derived collector array efficiency curve. The intersection of the average operating point for March and the March performance curve implied a monthly efficiency of 0.40. The exact agreement between the field derived collector array efficiency and the actual March monthly collector performance indicates that the field derived performance data could be used for design purposes.

Additional information concerning collector array analysis in general may be found in Reference [10]. The material in the reference describes the detailed collector array analysis procedures and presents the results of analyses performed on numerous collector array installations across the United States.

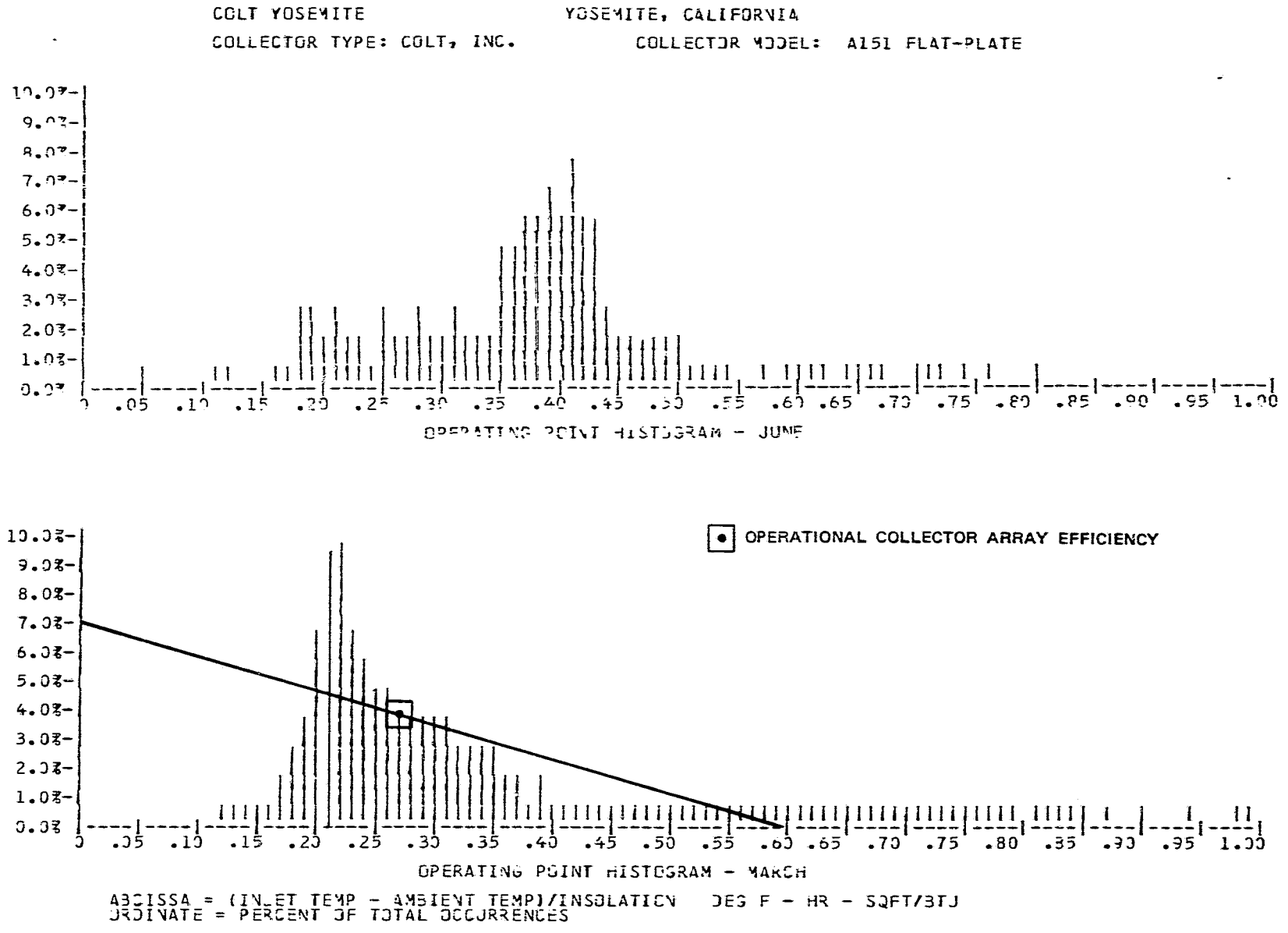

Figure 3.2.1-3 Colt Yosemite Operating Point Histograms for Typical Winter and Summer Months

3.2.2 Storage Subsystem

Storage subsystem performance is described by comparison of energy to storage, energy from storage and change in stored energy. The ratio of the sum of energy from storage and change in stored energy to energy to storage is defined as storage efficiency, η_s. This relationship is expressed in the equation

$$\eta_s = (\Delta Q + Q_{so})/Q_{si} \quad (8)$$

where:

ΔQ = Change in stored energy. This is the difference in the estimated stored energy during the specified reporting period, as indicated by the relative temperature of the storage medium (either positive or negative value)

Q_{so} = Energy from storage. This is the amount of energy extracted by the load subsystem from the primary storage medium

Q_{si} = Energy to storage. This is the amount of energy (both solar and auxiliary) delivered to the primary storage medium

Evaluation of the system storage performance under actual system operation and weather conditions can be performed using the parameters defined above. The utility of these measured data in evaluation of the overall storage design can be illustrated in the following discussion.

Table 3.2.2-1 summarizes the storage subsystem performance during the report period.

During the ten month period (July and August not included), a total of 83.51 million Btu was delivered to the storage tanks and a total of 63.84 million Btu was removed for support of system loads. The net change in stored energy during this same time period was -0.55 million Btu, which leads to a storage efficiency of 0.77 and a total energy loss from storage of 19.12 million Btu.

The computed storage efficiency of 0.77 is relatively high as compared to most solar energy systems. However, the average storage temperature during the period that efficiency was computed was only 100°F, so the high value of efficiency is not unrealistic. This is true because the potential for heat transfer becomes smaller as the differential temperature between the internal fluid and the external environment becomes smaller. However, this is not meant to detract in any way from the fact that the storage subsystem performed well during the reporting period. The system is well insulated and the effective heat transfer coefficient averaged only 72.55 Btu/Hr-°F during the period.

TABLE 3.2.2-1

STORAGE SUBSYSTEM PERFORMANCE

Month	Energy To Storage (Million Btu)	Energy From Storage (Million Btu)	Change In Stored Energy (Million Btu)	Storage Efficiency	Storage Average Temperature (°F)	Building Temp (°F)	Effective Storage Heat Loss Coefficient (Btu/Hr°F)
May 79	10.09	8.02	0.27	0.92	133	74	41.0
Jun 79	3.95	3.52	-1.22	0.58	126	78	47.7
Jul 79	0	0	-0.15	0	81	79	-
Aug 79	0	0	-0.12	0	76	74	-
Sep 79	3.33	1.66	1.25	0.87	80	74	94.1
Oct 79	6.78	6.36	-1.08	0.78	103	65	53.1
Nov 79	11.80	9.40	0.18	0.82	89	64	123.3
Dec 79	9.96	8.07	-0.08	0.80	89	63	101.8
Jan 80	8.39	6.91	0.10	0.84	88	64	77.3
Feb 80	8.70	7.17	0.68	0.90	97	65	38.2
Mar 80	12.28	5.44*	0.66	0.50	104	65	-
Apr 80	8.23	7.29	-1.04	0.76	132	70	44.4
Total	83.51	63.84	-0.55	-	-	-	-
Average	8.35	6.38	0.05	0.77	100	70	72.55

*Continous operation of the collector array between March 11 and March 20 resulted in the rejection of 6.05 million Btu from storage.

An effective storage heat transfer coefficient for the storage subsystem can be defined as follows:

$$C = (Q_{si} - Q_{so} - \Delta Q)/[(\bar{T}_s - \bar{T}_a) \times t] \frac{Btu}{Hr\text{-}^\circ F} \quad (9)$$

where

C = Effective storage heat transfer coefficient

Q_{si} = Energy to storage

Q_{so} = Energy from storage

ΔQ = Change in stored energy

$\bar{T}_s$ = Storage average temperature

$\bar{T}_a$ = Average ambient tempeature in the vicinity of storage

t = Number of hours in the month

The effective storage heat transfer coefficient is comparable to the heat loss rate defined in ASHRAE Standard 94-77 [9]. It has been calculated for each month in this report period and included, along with an assumed building average temperature, in Table 3.2.2-1.

Examination of the values for the effective storage heat transfer coefficient shows that the variation is quite significant. The liquid storage tank heat loss is highest during the coldest winter months and lowest during the spring and fall. Overall, the heat loss coefficient is quite low which is indicative of a properly performing liquid storage system.

The major source of liquid storage subsystem loss is the thermal energy transport system. For example, the thermal energy transport losses in February 1980 were 1.74 million Btu and the steady state thermal losses out of the liquid storage tank were 0.48 million Btu for a total indicated loss of 2.22 million Btu.

3.2.3 Space Heating Subsystem

The performance of the space heating subsystem is described by comparing the amount of solar energy supplied to the subsystem with the energy required to satisfy the total space heating load. The energy required to satisfy the total load consists of both solar energy and auxiliary thermal energy. The ratio of solar energy supplied to the load to the total load is defined as the heating solar fraction. The calculated heating solar fraction is the indicator of performance of the subsystem because it defines the percentage of the total space heating load supported by solar energy.

The performance of the Colt-Yosemite space heating subsystem is presented in Table 3.2.4-1. For the 12 month period from May 1979 through April 1980, the solar energy system supplied a total of 63.84 million Btu to the space heating load. The total heating load for this period was 277.23 million Btu, and the average monthly solar fraction was twenty-three percent. The contractor estimated that the solar system would provide enough solar energy to satisfy 56 percent of the heating demand. The actual results indicate that this cannot be achieved. If the solar system had operated optimally, a 28 percent solar fraction could be achieved and if losses which contribute to satisfying the space heating load are considered the greatest solar fraction would be on the order of 36 percent.

It must be emphasized that all values presented in this section relating to the performance of the space heating subsystem are based on measured parameters. In other words the space heating load, solar contribution and auxiliary thermal energy used are all determined based on the measured output of the space heating subsystem. These measured values do not include any of the various solar energy losses that are present in the system. However, solar energy losses are generally added to the interior of the building and, as such, represent an uncontrolled (unmeasured) contribution to the space heating load. At the Colt-Yosemite site these solar energy losses occur during energy transport between the various

TABLE 3.2.3-1

HEATING SUBSYSTEM PERFORMANCE

Month	Heating Parameters			Energy Consumed (Million Btu)			Measured Solar Fraction (Percent)
	Load (Million Btu)	Temperatures (°F)		Solar	Auxiliary Thermal	Auxiliary	
		Building	Outdoor				
May 79	9.44	74	59	8.02	1.41	2.36	85
Jun 79	3.52	78	66	3.52	0	0	100
Jul 79	0	79	72	0	0	0	100
Aug 79	0	74	70	0	0	0	100
Sep 79	1.66	74	70	1.66	0	0	100
Oct 79	15.60	65	56	6.36	9.24	15.41	41
Nov 79	49.03	64	44	9.40	39.63	66.05	19
Dec 79	39.87	63	41	8.07	31.80	53.00	20
Jan 80	36.38	64	41	6.91	29.47	49.11	19
Feb 80	33.47	65	44	7.17	26.30	43.83	21
Mar 80	47.77	65	44	5.44	42.36	70.56	11
Apr 80	40.49	70	51	7.29	33.20	55.33	18
Total	277.23			63.84	213.41	355.65	
Average	23.10	70	55	5.32	17.78	29.64	23

subsystems and, to a lesser extent, from the storage tank. These subsystems are located interior to the heated space. Thus, direct uncontrolled energy contribution can occur. The magnitude of the energy losses for the seasonal report period were 30.24 million Btu (collected energy measured - energy delivered to space heating). The solar energy contribution would then be 94.08 million Btu and the solar fraction of the space heating load 34 percent.

Figure 3.2.3-1 illustrates the measured building heat loss coefficient (UA), determined by ratioing the actual measured monthly space heating load to modified monthly degree-days multiplied by 24 [Modified degree days = actual degree days - (70 - building temperature) times the number of days in the month] The UA is highest in the fall months and reduces to a minimum value of 2512 Btu/Hr°F in January 1980. The indicated UA for this heating season averaged 3157 Btu/Hr-°F. The largest monthly discrepancy between the UA computed from this season and the past season was in September. Variation of the infiltration rates could very well account for this discrepancy.

A comparison of the measured building heat transfer coefficient, UA, and the predictions of the UA are shown in Figure 3.2.3-1. The system design load, which was utilized to size the solar energy system, was estimated to be 157,000 Btu/Hr. The estimated building UA can be obtained by using the local design temperature of 20°F. The UA estimated in this manner was 3488 Btu/Hr°F $\left[\frac{157{,}000 \text{ Btu/Hr}}{(65-20)°F} \right]$ which is very close to the UA determined from actual heating loads.

The design load estimation was accurate because actual building construction utilized poured concrete walls and typical auditorium roof construction which provides little insulation properties. Thus, the agreement between the actual and predicted UA's was expected. The difference between the building computed UA and measured UA is due to the contribution of significant solar energy system losses and to variations in infiltration rates.

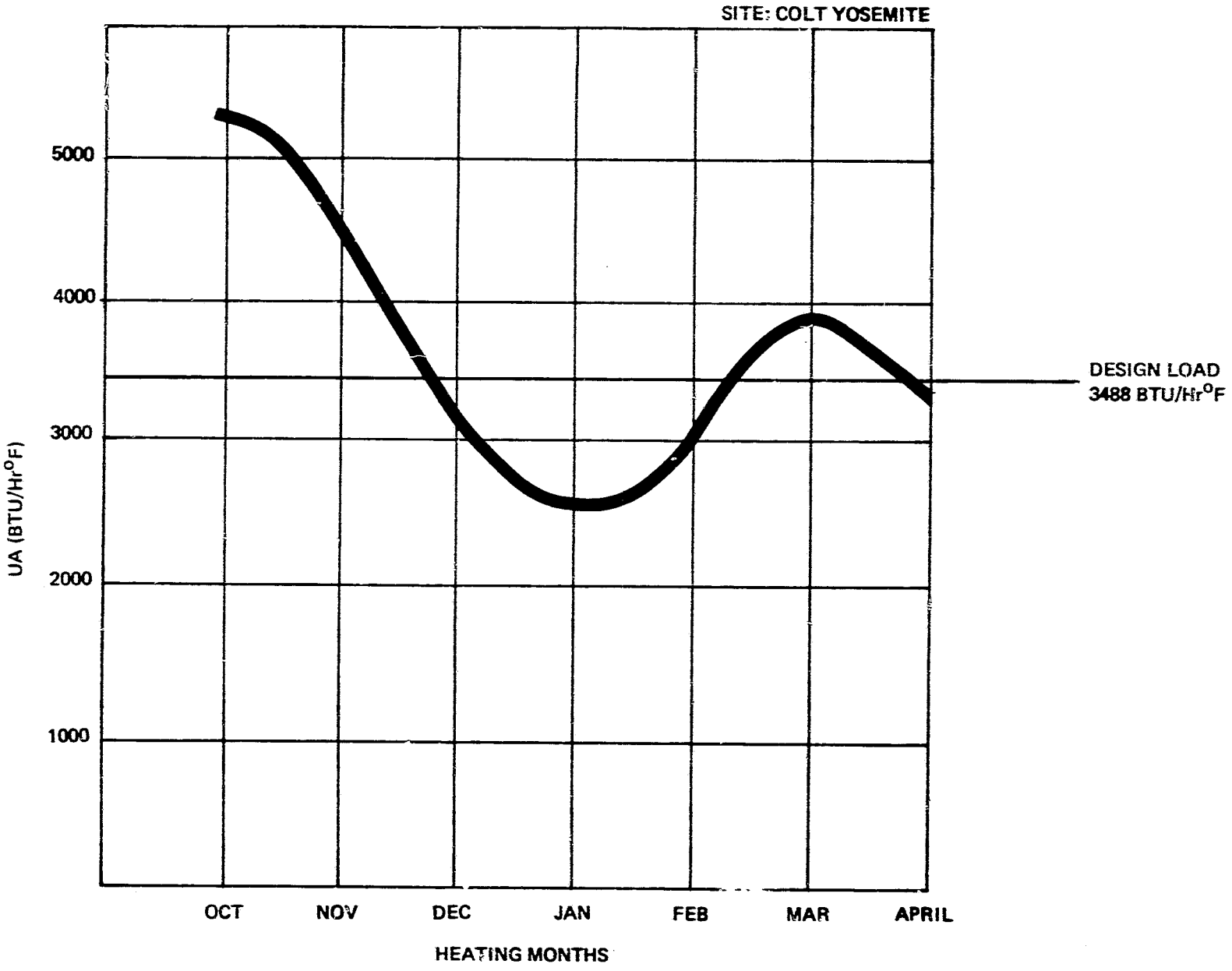

Figure 3.2.3-1 Building Heat Loss Coefficient

4. OPERATING ENERGY

Operating energy for the Colt-Yosemite Solar Energy System is defined as the energy required to transport solar energy to the point of use. Total operating energy for this system consists of energy collection and storage subsystem operating energy and space heating subsystem operating energy. Operating energy is electrical energy that is used to support the subsystems without affecting their thermal state. Measured monthly values for subsystem operating energy are presented in Table 4-1.

Total system operating energy for the Colt-Yosemite solar energy system is that electrical energy required to operate the pumps in the energy transport subsystem and the space circulating fan when solar energy is being utilized. These are shown as EP100, EP400, and EP600 respectively, in Figure 2-1. Although additional electrical energy is required to operate the valves in the energy transport subsystem and the control system for the installation, it is not included in this report. These devices are not monitored for power consumption and the power they consume is inconsequential when compared to the pump motor and fan motor powers.

During the 12 month reporting period, a total of 13.38 million Btu (3920 kWh) of operating energy was consumed. However, this includes the energy required to operate the blower in the auxiliary furnace, and that energy would be required whether or not the solar energy system was being utilized for space heating. Therefore, the energy consumed by the auxiliary furnace blower is not considered to be solar peculiar operating energy, even though it is included as part of the space heating subsystem operating energy.

TABLE 4-1

OPERATING ENERGY

Month	ECSS Operating Energy (Million Btu)	Space Heating Operating Energy (Million Btu)		Total System Operating Energy (Million Btu)
		Solar Pump	Circulating Fan	
May 79	0.71	0.36	0.60	1.67
Jun 79	0.34	0.18	0.28	0.80
Jul 79	0	0	0	0
Aug 79	0	0	0	0
Sep 79	0.19	0.13	0.19	0.51
Oct 79	0.44	0.27	0.43	1.14
Nov 79	0.65	0.53	0.79	1.97
Dec 79	0.59	0.47	0.69	1.75
Jan 80	0.43	0.35	0.51	1.29
Feb 80	0.46	0.32	0.46	1.24
Mar 80	1.36	0.21	0.33	1.90
Apr 80	0.49	0.23	0.39	1.11
Total	5.66	3.05	4.67	13.38
Average	0.47	0.25	0.39	1.12

A total of 8.71 million Btu (2552 kWh) of operating energy was required to support the pumps that are unique to the solar energy system during the reporting period. Of this total, 5.66 million Btu were allocated to the Energy Collection and Storage Subsystem (ECSS) and 3.05 million Btu were allocated to the solar portion of the Space Heating Subsystem. A total of 4.67 million Btu was allocated to the space heating circulating fan when the solar energy was being consumed. However, these additional energies are included in the total system operating energy. Since a measured 63.84 million Btu of solar energy was delivered to system loads during the reporting period, a total of 0.14 million Btu (40 kWh) of operating energy was required for each one million Btu of solar energy delivered to the system loads. The total space heating circulating fan energy for the seasonal period was 4.67 million Btu (1369 kWh).

5. ENERGY SAVINGS

Solar energy system savings are realized whenever energy provided by the solar energy system is used to meet system demands which would otherwise be met by auxiliary energy sources. The operating energy required to provide solar energy to the load subsystems is subtracted from the solar energy contribution, and the resulting energy savings are adjusted to reflect the coefficient of performance (COP) of the auxiliary source being supplanted by solar energy.

The Colt-Yosemite auxiliary energy system has a fuel oil boiler located in the main heating plant associated with the Yosemite National Park. Energy from this boiler is transmitted to a heat exchanger located in the auditorium supply ducting. The circulating fan then distributes this energy to the building. For computational purposes the fuel oil furnace is considered to be 60 percent efficient. Energy savings for the 12 month reporting period are presented in Table 5-1. Fossil fuel savings for the reporting period totaled 109.92 million Btu, or 785 gallons of fuel oil (based on a heating value of 140,000 Btu per gallon). The total savings in fossil equivalent at the source of energy generation was 80.89 million Btu, or 578 gallons of fuel oil. The reduction in fossil savings is due to the cost of operating the solar system. If the losses of 30.24 million Btu are considered as meeting the space heating demand, the overall fossil fuel savings rises to 111.13 million Btu, or 794 gallons of fuel oil.

TABLE 5-1

ENERGY SAVINGS

Month	Fossil Energy Savings (Million Btu) Space Heating	Solar Operating Energy (Million Btu)	Net Savings			Fossil * Equivalent At Source (Million Btu)
			Electrical		Fossil	
			Million Btu	kWh	Million Btu	
May 79	15.67	1.07	-1.07	-313.5	15.67	12.10
Jun 79	5.86	0.52	-0.52	-152.4	5.86	4.13
Jul 79	0	0	0	0	0	0
Aug 79	0	0	0	0	0	0
Sep 79	3.99	0.32	-0.32	-93.8	3.99	2.92
Oct 79	10.60	0.71	-0.71	-208.0	10.60	8.23
Nov 79	15.66	1.18	-1.18	-345.7	15.66	11.73
Dec 79	13.45	1.06	-1.06	-310.6	13.45	9.92
Jan 80	11.52	0.78	-0.78	-228.5	11.52	8.92
Feb 80	11.96	0.78	-0.78	-228.5	11.96	9.36
Mar 80	9.06	1.57	-1.57	-459.4	9.06	3.23
Apr 80	12.15	0.72	-0.72	-211.0	12.15	9.75
Total	109.92	8.71	-8.71	-2551.4	109.92	80.89
Average	9.16	0.73	-0.73	-212.6	9.16	6.74

*Fossil savings equivalent at source = Fossil Savings -(Solar Operating Energy/ 0.3)

6. MAINTENANCE

A considerable amount of maintenance was required at the Colt-Yosemite site since activation.

The solar energy collectors were replaced during October due to extensive leakage and the flow meters were returned for recalibration.

Power station dropouts (voltage below 85 VAC) occurred intermittently during October and November 1979. These dropouts ceased to exist after these months.

In December and January, collector loop pump cavitation resulted in little, if any, solar energy usage during those months. The situation was repaired in late January.

The solar energy space heating flow sensor was reinstalled on December 12, 1978.

The auxiliary flow meter W401 was reinstalled on February 8, 1979. However, after a brief observation period it was determined that the flow meter range was again insufficient and it was returned for recalibration on 3/22/79. The sensor was again installed on May 9, 1979 and a wiring error corrected later in the month.

Pollen deposited on the collectors during the spring was so extensive that insolation was reduced 15 percent. Attempts to clean the collectors were to no avail. The collectors were leaking so badly that a decision was made to replace the entire array in the later part of the summer of 1979.

The insolation pyranometer was raised 8 ft. vertically in an attempt to prevent local pine trees from shading the instrument. The shading effect was reduced but not entirely eliminated.

Between September and early November, the new collector array was installed and the collector transport fluid changed to Diala-Ax oil. The array was operational November 5, 1979.

An evaluation of the auxiliary heat exchanger operation on site was performed and instrumentation associated with this subsystem verified as being correct. The system is being operated at below normal flow which also creates large temperature differentials. This type of operation is detrimental to operation of this subsystem and also provides difficulty in accurately measuring auxiliary consumption.

Several banks of collectors were removed (11 collectors) for three weeks in December to facilitate repairs to the system. This caused a performance reduction during the month.

In late December, the auxiliary flow changed characteristics from a normal cyclical nature to a low level continuous output. The cause for the change was due to sticking of the 3-way valve associated with the subsystem. This condition made it difficult to measure auxiliary consumption accurately because of the low signal to noise ratio that existed in the output of the water flow meter W401.

An auxiliary pump failure prevented normal operation of the solar system during January 1980.

Three collectors were permanently removed on December 22, 1979 and another on March 9, 1979 due to excessive leakage.

An overpressure condition in the solar system transport piping has caused extensive damage to the solar system. Extensive repairs are being made to the system.

7. SUMMARY AND CONCLUSIONS

Yosemite National Park is located in the lofty Sierra Nevada mountains. The most popular area in the park is the 7-square mile Yosemite Valley, famous for its sheer walls, waterfalls, towering domes and mountain peaks high above the valley floor. The Yosemite visitors center is located in this valley. Several large pine trees are located near the visitor's center which provide natural beauty but also shade the building. The combination of pine trees and cliffs cause significant solar system performance penalties which prevented the system from performing up to expectations. The system was expected to provide 56 percent of the space heating demand of the auditorium associated with the visitor's center.

During the 12 month reporting period, the measured daily average incident insolation in the plane of the collector array was 1,473 Btu/Ft^2. This was nine percent below the long-term daily average of 1,622 Btu/Ft^2 after considering known shading effects. The measured insolation appears to be an accurate representation of the long-term average for the valley. Both the long-term averages for ambient temperature and insolation are derived from an average of data taken from Davis and in Inyokern, California. During the period from May, 1979, through April, 1980, the measured average outdoor ambient temperature was 55°F. This was one degree above the long term average of 54°F for the same period. As a result, 4,381 heating degree-days were accumulated, as compared to the long-term average of 4,507 heating degree-days.

The solar energy system satisfied 23 percent of the total measured load during the 12 month reporting period. This was significantly below the design value of 56 percent estimated by Colt, Inc. [1]. The reduction in overall system solar fraction was due primarily to the large building heat loss associated with the visitor's center and to the measured performance of the space heating subsystem. The space

heating solar fraction for the reporting period was 23 percent. However, the computations do not account for uncontrolled losses of solar energy into the building that result primarily from transport piping losses. As discussed in Section 3.2.3, these losses are substantial and provide a considerable contribution to the measured space heating load. However, even if all the losses were considered to have contributed to the space heating load the solar fraction achievable would be 34 percent.

A total of 514.77 million Btu of incident solar energy was measured in the plane of the collector array during the reporting period. The system collected 94.08 million Btu of the available energy, which represents a collector array efficiency of 23 percent. During periods when the collector array was active, a total of 257.00 million Btu was measured in the plane of the collector array. Therefore, the operational collector efficiency was 37 percent. Taking into account the heat exchanger penalty factor, the collector array performance was close to that expected.

During the reporting period, a total of 63.84 million Btu of solar energy was delivered to the storage tanks. All of this (63.84 million Btu) went to the space heating subsystem. The effective storage tank loss coefficient was 72.55 Btu/Hr-°F, which is low and indicates a well insulated storage subsystem. The average temperature of storage was 100°F for the period.

A total of 13.38 million Btu, or 3920 kWh, of electrical operating energy was required to support the solar energy system during the 12 month reporting period. This includes the electrical energy required to operate the circulating fan in the auxiliary furnace. This fan would be required for operation of the space heating subsystem regardless of the presence of the solar energy system. The circulating fan energy is 4.67 million Btu.

Fossil energy savings for the 12 month reporting period were 109.92 million Btu. The solar electrical operating energy was 8.71 million Btu, or 2552 kWh. If a 30 percent efficiency is assumed for power generation and distribution, then the net electrical energy translate into a cost of 29.02 million Btu in generating station fuel requirements. Thus, the overall equivalent fossil savings at the source of energy generation was 80.89 million Btu or 578 gallons of fuel oil assuming a conversion factor of 140,000 Btu/gallon. It should also be noted that the fossil energy savings are based only on the measured amount of solar energy delivered to the space heating subsystem. As discussed in Section 3.2.4, the fossil energy savings will increase considerably if the uncontrolled solar energy input to the building is considered.

In general, the performance of the Colt-Yosemite Solar Energy System performed below normal during the reporting time period. The substantial maintenance necessary to maintain the system with resultant down time combined with below normal insolation is the cause of the performance reduction. However, it must be again stressed that the measured heating subsystem performance does not include the uncontrolled addition of solar energy to the building. If the uncontrolled losses could have been reduced to an inconsequential level, then both the measured system performance and the accuracy of the system analysis would have improved considerably.

8. REFERENCES

1. NASA-8-32242, System Performance Specification (SHC-3025), July 12, 1979.

2. NASA/DOE CR-150760, Installation Package for a Domestic Solar Heating and Hot Water System, August 1978.

3. Colt Solar Brochure, Colt, Inc., Energy Systems Division, 71-590 San Jacinto, Rancho Mirage, CA.

4. Preliminary Evaluation Results of the Collector Array Performance of the Colt, Inc. Operational Test Sites at Yosemite, CA (OTS-1) and Pueblo CO (OTS-2), memo by Rufus D. Collins, Jr. of MSFC [EL51].

5. De Winter, F., Heat Exchanger Penalties in Double-Loop Solar Water Heating Systems, Solar Energy Vol. 17, pp 335-337, 1975.

6. E. Streed, etc. al., Thermal Data Requirements and Performance Evaluation Procedures for the National Solar Heating and Cooling Demonstration Program, NBSIR-76-1137, National Bureau of Standards, Washington, August, 1976.

7. J. T. Smok, V. S. Sohoni, J. M. Nash, "Processing of Instrumented Data for the National Solar Heating and Cooling Demonstration Program", Conference on Performance Monitoring Techniques for Evaluation of Solar Heating and Cooling Systems, Washington, D. C., April, 1978.

8. ASHRAE Standard 93-77, Methods of Testing to Determine the Thermal Performance of Solar Collectors, The American Society of Heating Refrigeration and Air Conditioning Engineers, Inc., New York, NY, 1977.

9. ASHRAE Standard 94-77, Methods of Testing Thermal Storage Devices Based on Thermal Performance, The American Society of Heating Refrigeration and Air Conditioning Engineers, Inc., New York, NY 1977.

10. McCumber, W. H. Jr., "Collector Array Performance for Instrumented Sites of the National Solar Heating and Cooling Demonstration Program," published and distributed at the 1979 Solar Update Conference.

11. Beckman, William A.; Klein, Sanford A; Duffie, John A.; Solar Heating Design by the f-Chart Method, Wiley Interscience New York, NY, 1977.

APPENDIX A

DEFINITION OF PERFORMANCE FACTORS

AND

SOLAR TERMS

APPENDIX A
DEFINITION OF PERFORMANCE FACTORS AND SOLAR TERMS

COLLECTOR ARRAY PERFORMANCE

The collector array performance is characterized by the amount of solar energy collected with respect to the energy available to be collected.

- INCIDENT SOLAR ENERGY (SEA) is the total insolation available on the gross collector array area. This is the area of the collector array energy-receiving aperture, including the framework which is an integral part of the collector structure.

- OPERATIONAL INCIDENT ENERGY (SEOP) is the amount incident solar energy on the collector array during the time that the collector loop is active (attempting to collect energy).

- COLLECTED SOLAR ENERGY (SECA) is the thermal energy removed from the collector array by the energy transport medium.

- COLLECTOR ARRAY EFFICIENCY (CAREF) is the ratio of the energy collected to the total solar energy incident on the collector array. It should be emphasized that this efficiency factor is for the collector array, and available energy includes the incident energy on the array when the collector loop is inactive. This efficiency must not be confused with the more common collector efficiency figures which are determined from instantaneous test data obtained during steady state operation of a single collector unit. These efficiency figures are often provided by collector manufacturers or presented in technical journals to characterize the functional capability of a particular collector design. In general, the collector panel maximum efficiency factor will be significantly higher than the collector array efficiency reported here.

STORAGE PERFORMANCE

The storage performance is characterized by the relationships among the energy delivered to storage, removed from storage, and the subsequent change in the amount of stored energy.

- ENERGY TO STORAGE (STEI) is the amount of energy, both solar and auxiliary, delivered to the primary storage medium.

- ENERGY FROM STORAGE (STEO) is the amount of energy extracted by the load subsystems from the primary storage medium.

- CHANGE IN STORED ENERGY (STECH) is the difference in the estimated stored energy during the specified reporting period, as indicated by the relative temperature of the storage medium (either positive or negative value).

- STORAGE AVERAGE TEMPERATURE (TST) is the mass-weighted average temperature of the primary storage medium.

- STORAGE EFFICIENCY (STEFF) is the ratio of the sum of the energy removed from storage and the change in stored energy to the energy delivered to storage.

ENERGY COLLECTION AND STORAGE SUBSYSTEM

The Energy Collection and Storage Subsystem (ECSS) is composed of the collector array, the primary storage medium, the transport loops between these, and other components in the system design which are necessary to mechanize the collector and storage equipment.

- INCIDENT SOLAR ENERGY (SEA) is the total insolation available on the gross collector array area. This is the area of the collector array energy-receiving aperture, including the framework which is an integral part of the collector structure.

- AMBIENT TEMPERATURE (TA) is the average temperature of the outdoor environment at the site.

- ENERGY TO LOADS (SEL) is the total thermal energy transported from the ECSS to all load subsystems.

- AUXILIARY THERMAL ENERGY TO ECSS (CSAUX) is the total auxiliary energy supplied to the ECSS, including auxiliary energy added to the storage tank, heating devices on the collectors for freeze-protection, etc.

- ECSS OPERATING ENERGY (CSOPE) is the critical operating energy required to support the ECSS heat transfer loops.

SPACE HEATING SUBSYSTEM

The space heating subsystem is characterized by performance factors accounting for the complete energy flow to and from the subsystem. The average building temperature and the average ambient temperature are tabulated to indicate the relative performance of the subsystem in satisfying the space heating load and in controlling the temperature of the conditioned space.

- SPACE HEATING LOAD (HL) is the sensible energy added to the air in the building.

- SOLAR FRACTION OF LOAD (HSFR) is the fraction of the sensible energy added to the air in the building derived from the solar energy system.

- SOLAR ENERGY USED (HSE) is the amount of solar energy supplied to the space heating subsystem.

- OPERATING ENERGY (HOPE) is the amount of electrical energy required to support the subsystem, (e.g., fans, pumps, etc.) and which is not intended to affect directly the thermal state of the subsystem.

- AUXILIARY THERMAL USED (HAT) is the amount of energy supplied to the major components of the subsystem in the form of thermal energy in a heat transfer fluid or its equivalent. This term also includes the converted electrical and fossil fuel energy supplied to the subsystem.

- AUXILIARY FOSSIL FUEL (HAF) is the amount of fossil energy supplied directly to the subsystem.

- FOSSIL ENERGY SAVINGS (HSVF) is the estimated difference between the fossil energy requirements of an alternative conventional system (carrying the full load) and the actual fossil energy required by the subsystem.

- ELECTRICAL ENERGY SAVINGS (HSVE) is the cost of the operating energy (HOPE) required to support the solar energy portion of the space heating subsystem.

- BUILDING TEMPERATURE (TB) is the average heated space dry bulb temperature.

- AMBIENT TEMPERATURE (TA) is the average ambient dry bulb temperature at the site.

ENVIRONMENTAL SUMMARY

The environmental summary is a collection of the weather data which is generally instrumented at each site in the program. It is tabulated in this data report for two purposes--as a measure of the conditions prevalent during the operation of the system at the site, and as an historical record of weather data for the vicinity of the site.

- TOTAL INSOLATION (SE) is accumulated total incident solar energy upon the gross collector array measured at the site.

- AMBIENT TEMPERATURE (TA) is the average temperature of the environment at the site.

- WIND DIRECTION (WDIR) is the average direction of the prevailing wind.

- WIND SPEED (WIND) is the average wind speed measured at the site.

- DAYTIME AMBIENT TEMPERATURE (TDA) is the temperature during the period from three hours before solar noon to three hours after solar noon.

APPENDIX B

SOLAR ENERGY SYSTEM PERFORMANCE EQUATIONS

COLT-YOSEMITE

APPENDIX B

SOLAR ENERGY SYSTEM PERFORMANCE EQUATIONS FOR COLT-YOSEMITE

I. INTRODUCTION

Solar energy system performance is evaluated by performing energy balance calculations on the system and its major subsystems. These calculations are based on physical measurement data taken from each subsystem every 320 seconds. This data is then numerically combined to determine the hourly, daily, and monthly performance of the system. This appendix describes the general computational methods and the specific energy balance equations used for this evaluation.

Data samples from the system measurements are numerically integrated to provide discrete approximations of the continuous functions which characterize the system's dynamic behavior. This numerical integration is performed by summation of the product of the measured rate of the appropriate performance parameters and the sampling interval over the total time period of interest.

There are several general forms of numerical integration equations which are applied to each site. Examples of these general forms are as follows: The total solar energy available to the collector array is given by

$$\text{SOLAR ENERGY AVAILABLE} = (1/60)\ \Sigma\ [\text{I001} \times \text{AREA}] \times \Delta\tau$$

where I001 is the solar radiation measurement provided by the pyranometer in Btu/ft^2-hr, AREA is the area of the collector array in square feet, $\Delta\tau$ is the sampling interval in minutes, and the factor (1/60) is included to correct the solar radiation "rate" to the proper units of time.

Similarly, the energy flow within a system is given typically by

$$\text{COLLECTED SOLAR ENERGY} = \Sigma\ [M100 \times \Delta H] \times \Delta\tau$$

where M100 is the mass flow rate of the heat transfer fluid, in lb_m/min, and ΔH is the enthalpy change, in Btu/lb_m, of the fluid as it passes through the heat exchanging component.

For a liquid system ΔH is generally given by

$$\Delta H = \bar{C}_p\ \Delta T$$

where $\bar{C}_p$ is the average specific heat, in $Btu/(lb_m\text{-}°F)$, of the heat transfer fluid and ΔT, in °F, is the temperature differential across the heat exchanging component.

For an air system ΔH is generally given by

$$\Delta H = H_a(T_{out}) - H_a(T_{in})$$

where $H_a(T)$ is the enthalpy, in Btu/lb_m, of the transport air evaluated at the inlet and outlet temperatures of the heat exchanging component.

$H_a(T)$ can have various forms, depending on whether or not the humidity ratio of the transport air remains constant as it passes through the heat exchanging component.

For electrical power, a general example is

$$\text{ECSS OPERATING ENERGY} = (3413/60)\ \Sigma\ [EP100] \times \Delta\tau$$

where EP100 is the measured power required by electrical equipment in kilowatts and the two factors (1/60) and 3413 correct the data to Btu/min.

These equations are comparable to those specified in "Thermal Data Requirements and Performance Evaluation Procedures for the National Solar Heating and Cooling Demonstration Program." This document, given in the list of references, was prepared by an inter-agency committee of the government, and presents guidelines for thermal performance evaluation.

Performance factors are computed for each hour of the day. Each numerical integration process, therefore, is performed over a period of one hour. Since long-term performance data is desired, it is necessary to build these hourly performance factors to daily values. This is accomplished, for energy parameters, by summing the 24 hourly values. For temperatures, the hourly values are averaged. Certain special factors, such as efficiencies, require appropriate handling to properly weight each hourly sample for the daily value computation. Similar procedures are required to convert daily values to monthly values.

II. PERFORMANCE EQUATIONS

The performance equations for Colt-Yosemite used for the data evaluation of this report are contained in the following pages and have been included for technical reference and information.

EQUATIONS USED IN MONTHLY PERFORMANCE ASSESSMENT

NOTE: MEASUREMENT NUMBERS REFERENCE SYSTEM SCHEMATIC FIGURE 2-1

AVERAGE AMBIENT TEMPERATURE (°F)

$$TA = (1/60) \times \Sigma\ T001 \times \Delta\tau$$

AVERAGE BUILDING TEMPERATURE (°F)

$$TB = (1/60) \times \Sigma\ T600 \times \Delta\tau$$

DAYTIME AVERAGE AMBIENT TEMPERATURE (°F)

$$TDA = (1/360) \times \Sigma\ T001 \times \Delta\tau$$

FOR $\pm$ 3 HOURS FROM SOLAR NOON

INCIDENT SOLAR ENERGY PER SQUARE FOOT (BTU/FT^2)

$$SE = (1/60) \times \Sigma\ I001 \times \Delta\tau$$

OPERATIONAL INCIDENT SOLAR ENERGY (BTU)

$$SEOP = (1/60) \times \Sigma\ [I001 \times CLAREA] \times \Delta\tau$$

WHEN THE COLLECTOR LOOP IS ACTIVE

SOLAR ENERGY COLLECTED BY THE ARRAY (BTU)

$$SECA = \Sigma\ [M100 \times CP46\ (0.5 \times (T101 + T151)) \times (T151 - T101)] \times \Delta\tau$$

WHERE CP46 ( ) IS SPECIFIC HEAT OF COLLECTOR TO STORAGE ENERGY TRANSFER FLUID (SHELL 33 OR DIALA-AX 33).

ENTHALPY FUNCTION FOR WATER (BTU/LBM)

$$HWD(T_2, T_1) = \int_{T_1}^{T_2} C_p(T)dT$$

THIS FUNCTION COMPUTES THE ENTHALPY CHANGE OF WATER AS IT PASSES THROUGH A HEAT EXCHANGING DEVICE.

SOLAR ENERGY TO STORAGE (BTU)

$$STEI = \Sigma\ [M100 \times CP46\ (0.5 \times (T100 + T150)) \times (T150 - T100)] \times \Delta\tau$$

SOLAR ENERGY FROM STORAGE TO SPACE HEATING (BTU)

$$STEO = \Sigma\ [M400 \times HWD\ (T451, T401)] \times \Delta\tau$$

AVERAGE TEMPERATURE OF STORAGE (°F)

$$TSTM = (T200 + T201 + T202)/3$$

$$TSTL = TSTM$$

$$TST = TSTM \times (1/60)$$

ENERGY DELIVERED FROM ECSS TO LOAD SUBSYSTEMS (BTU)

$$CSEO = STEO$$

ECSS OPERATING ENERGY (BTU)

$$CSOPE = 56.8833 \times \Sigma\ EP100 \times \Delta\tau$$

SPACE HEATING SUBSYSTEM SOLAR OPERATING ENERGY (BTU)

$$HOPE1 = 56.8833 \times \Sigma\ EP400 \times \Delta\tau$$

SOLAR ENERGY TO SPACE HEATING SUBSYSTEM (BTU)

$$HSE = STEO$$

AUXILIARY FOSSIL ENERGY TO SPACE HEATING SUBSYSTEM (BTU)

$$HAT = \Sigma\ [M401 \times HWD\ (T452, T402)] \times \Delta\tau$$

SPACE HEATING CIRCULATING FAN ENERGY (BTU)

$$HOPEA = 56.8833 \times \Sigma\ EP600 \times \Delta\tau$$

SPACE HEATING SUBSYSTEM OPERATING ENERGY (BTU)

$$HOPE = HOPEA + HOPE1$$

INCIDENT SOLAR ENERGY ON COLLECTOR ARRAY (BTU)

SEA = CLAREA x SE

COLLECTED SOLAR ENERGY (BTU/FT^2)

SEC = SECA/CLAREA

COLLECTOR ARRAY EFFICIENCY

CAREF = SECA/SEA

CHANGE IN STORED ENERGY (BTU)

STECH1 = STOCAP x TSTL x CP (TSTL) x RHO (TSTL)

STECH = $STECH1 - STECH1_p$

WHERE THE SUBSCRIPT $_p$ REFERS TO A PRIOR REFERENCE VALUE

STORAGE EFFICIENCY

STEFF = (STECH + STEO)/STEI

SOLAR ENERGY TO LOAD SUBSYSTEMS (BTU)

SEL = HSE

ECSS SOLAR CONVERSION EFFICIENCY

CSCEF = CSEO/SEA

AUXILIARY FOSSIL FUEL (BTU)

HAF = HAT/0.6

SPACE HEATING LOAD (BTU)

HL = HAT + HSE

SPACE HEATING SUBSYSTEM SOLAR FRACTION (PERCENT)

HSFR = 100 x HSE/HL

SPACE HEATING SUBSYSTEM ELECTRICAL ENERGY SAVINGS (BTU)

HSVE = -HOPE1

SPACE HEATING SUBSYSTEM FOSSIL ENERGY SAVINGS (BTU)

HSVF = HSE/0.6

SYSTEM LOAD (BTU)

SYSL = HL + HWL

SOLAR FRACTION OF SYSTEM LOAD (PERCENT)

SFR = (HL x HSFR + HWL x HWSFR)/SYSL

SYSTEM OPERATING ENERGY (BTU)

SYSOPE = CSOPE + HOPE

AUXILIARY THERMAL ENERGY TO LOADS (BTU)

AXT = HAT

AUXILIARY FOSSIL ENERGY TO LOADS

AXF = HAF

TOTAL ELECTRICAL ENERGY SAVINGS (BTU)

TSVE = HSVE - CSOPE

TOTAL FOSSIL ENERGY SAVINGS (BTU)

TSVF = HSVF

TOTAL ENERGY CONSUMED (BTU)

TECSM = SYSOPE + SECA + AXF

SYSTEM PERFORMANCE FACTOR

SYSPF = SYSL/(AXF + SYSOPE x 3.33)

NEGSECA

IF EP600 >0 AND (T101 - T151) >0

THEN NEGSECA = Σ [M100 * CP46 (0.5 x (T101 + T151) x

(T101 - T151)] x $\Delta\tau$

STL2

IF EP400 > 0 & (T200 - T451) > 0

THEN STL2 = Σ [M400 x (T200 - T451)] x $\Delta\tau$

SPACE HEATING TRANSPORT LOSSES ESTIMATION

$$AHL = \Sigma\ [76.34 \times ((T401 + T451)/2 - TB) \times (0.21 + 5.E\text{-}4 \times TST)] \times \Delta\tau$$

SOLAR TANK STATIC HEAT LOSS ESTIMATION

$$STL = \Sigma\ [26.85 \times ((T200 + T201 + T202)/3 - TB)] \times \Delta\tau$$

APPENDIX C

LONG TERM AVERAGE WEATHER CONDITIONS

APPENDIX C

LONG-TERM AVERAGE WEATHER CONDITIONS

The environmental estimates given in this appendix provide a point of reference for evaluation of weather conditions as reported in the Monthly Performance Reports and Solar Energy System Performance Evaluations issued by the Solar Heating, Cooling and Hot Water Development Program. As such, the information presented can be useful in prediction of long-term system performance.

Environmental estimates for this site include the following monthly averages: extraterrestrial insolation, insolation on a horizontal plane at the site, insolation in the tilt plane of the collection surface, ambient temperature, heating degree-days, and cooling degree-days. Estimation procedures and data sources are detailed in the following paragraphs.

The preferred source of long-term temperature and insolation data is "Input Data for Solar Systems" (IDSS) [1] since this has been recognized as the solar standard. The IDSS data are used whenever possible in these environmental estimates for both insolation and temperature related sources; however, a secondary source used for insolation data is the Climatic Atlas of the United States [2], and for temperature related data, the secondary source is "Local Climatological Data" [3].

Since the available long-term insolation data are only given for a horizontal surface, solar collection subsystem orientation information is used in an algorithm [4] to calculate the insolation expected in the tilt plane of the collector. This calculation is made using a ground reflectance of 0.2.

SITE: COLT YOSEMITE 44. LOCATION: YOSEMITE NP CA

ANALYST: K. SHENFISH FDRIVE NO.: 62.

COLLECTOR TILT: 50.00 (DEGREES) COLLECTOR AZIMUTH: 20.00 (DEGREES)

LATITUDE: 37.50 (DEGREES) RUN DATE: 04/29/80

MONTH	HOBAR	HBAR	KBAR	RBAR	SBAR	HDD	CDD	TBAR
JAN	1460.	819.	0.560951	1.756	1437.	813	0	39.
FEB	1914.	1154.	0.602609	1.474	1701.	626	0	43.
MAR	2490.	1539.	0.618442	1.208	1966.	584	0	46.
APR	3076.	2098.	0.682124	0.975	2046.	399	0	52.
MAY	3476.	2408.	0.692657	0.822	1979.	234	10	58.
JUN	3635.	2595.	0.711104	0.758	1959.	102	[illegible]	64.
JUL	3549.	2526.	0.711756	0.785	1983.	37	144	68.
AUG	3225.	2260.	0.700971	0.907	2050.	41	115	67.
SEP	2697.	1864.	0.690947	1.113	2107.	85	54	64.
OCT	2030.	1379.	0.680297	1.404	1935.	280	11	56.
NOV	1565.	933.	0.596410	1.698	1584.	540	0	47.
DEC	1335.	745.	0.558080	1.861	1386.	765	0	40.

LEGEND:

HOBAR ==> MONTHLY AVERAGE DAILY EXTRATERRESTRIAL RADIATION (IDEAL) IN BTU/DAY-FT2.

HBAR ==> MONTHLY AVERAGE DAILY RADIATION (ACTUAL) IN BTU/DAY-FT2.

KBAR ==> RATIO OF HBAR TO HOBAR.

RBAR ==> RATIO OF MONTHLY AVERAGE DAILY RADIATION ON TILTED SURFACE TO THAT ON A HORIZONTAL SURFACE FOR EACH MONTH (I.E., MULTIPLIER OBTAINED BY TILTING).

SBAR ==> MONTHLY AVERAGE DAILY RADIATION ON A TILTED SURFACE (I.E., RBAR * HBAR) IN BTU/DAY-FT2.

HDD ==> NUMBER OF HEATING DEGREE DAYS PER MONTH.

CDD ==> NUMBER OF COOLING DEGREE DAYS PER MONTH.

TBAR ==> AVERAGE AMBIENT TEMPERATURE IN DEGREES FAHRENHEIT.

REFERENCES

[1] Cinquemani, V., et al. "Input Data for Solar Systems." Prepared for the U.S. Department of Energy by the National Climatic Center, Asheville, NC, 1978.

[2] United States Department of Commerce, Climatic Atlas of the United States, Environmental Data Service, Reprinted by the National Oceanic and Atmospheric Administration, Washington, DC, 1977.

[3] United States Department of Commerce, "Local Climatological Data," Environmental Data Service, National Oceanic and Atmospheric Administration, Asheville, NC, 1977.

[4] Klein, S. A., "Calculation of Monthly Average Insolation on Tilted Surfaces," Joint Conference 1976 of the International Solar Energy Society and the Solar Energy Society of Canada, Inc., Winnipeg, August 15-20, 1976.

U.S. GOVERNMENT PRINTING OFFICE 1980—640-247/103 REGION NO.4